Invited Review submitted for Publication in
Advances in Biochemical Engineering / Biotechnology

In Vivo Stationary Flux Analysis by ^{13}C Labeling Experiments

W. Wiechert, A.A. de Graaf
Institut für Biotechnologie, Forschungszentrum Jülich
D-52425 Jülich, Germany

Abstract:

Stationary flux analysis is an invaluable tool for metabolic engineering. In the last years the metabolite balancing technique has become well established in the bioengineering community. On the other hand metabolic tracer experiments using ^{13}C isotopes have long been used for intracellular flux determination. Only recently both techniques have been combined in full extent to form a considerably more powerful flux analysis method. This paper concentrates on modeling and data analysis for the evaluation of such stationary ^{13}C labeling experiments. After reviewing the recent experimental developments the basic equations for modeling carbon labeling in metabolic systems, i.e. metabolite, carbon label and isotopomer balances are introduced and discussed in some detail. Then the basics of flux estimation from measured extracellular fluxes combined with carbon labeling data are presented and finally this method is illustrated by using an example from *C. glutamicum*. Main emphasis lays on the investigation of the excess information that can be obtained with tracer experiments compared with the metabolite balancing technique alone. As a principal result it is shown that the combined flux analysis method can dispense with some rather doubtful assumptions on energy balancing and moreover, that the forward and backward flux rates of bidirectional reaction steps can be simultaneously determined in certain situations. Finally, it is demonstrated that the variant of fractional isotopomer measurement is even more powerful than fractional labeling measurement but requires much higher numerical efforts for solving the balance equations.

Contents

List of Symbols:

A,B,C,D,E,S,P,...	metabolite names
$A, B, C, D, E, S, P, \ldots$	absolute molar pool size of metabolites
b_1, b_2	positional fractional carbon labeling of metabolite B with 2 carbon atoms
$b_{00}, b_{01}, b_{10}, b_{11}$	isotopomer fractions of metabolite B with 2 carbon atoms
$v_1^{\rightarrow}, v_1^{\leftarrow}, v_2^{\rightarrow}, v_2^{\leftarrow}$	forward and backward fluxes corresponding to biochemical reaction steps
$\mathbf{x}, \mathbf{x}^{\text{inp}}$	vectors of all fractional carbon labels in a metabolic network and all input labels from substrates fed into the system
$\mathbf{X}$	vector of all absolute pool sizes in a metabolic network
$\mathbf{v}^{\rightarrow}, \mathbf{v}^{\leftarrow}$	vectors of all forward and backward fluxes corresponding to metabolic reaction steps
$\mathbf{v}$	overall flux vector comprising $\mathbf{v}^{\rightarrow}$ and $\mathbf{v}^{\leftarrow}$
$\mathbf{v}^{\text{net}}, \mathbf{v}^{\text{xch}}$	vectors of all net and exchange fluxes corresponding to metabolic reaction steps
$\mathbf{N}$	stoichiometric matrix
$\mathbf{N}^{\text{cnstr}}, \mathbf{c}^{\text{cnstr}}$	linear constraint matrix and constraint value vector
$\mathbf{P}_i, \mathbf{P}_i^{\text{inp}}$	carbon atom transition matrices corresponding to reaction step i
$\mathbf{Q}_i$	bimolecular isotopomer transition tensor corresponding to reaction step i
$\mathbf{I}$	pool size to fractional labeling state mapping matrix
$\mathbf{w}, \mathbf{y}, \mathbf{Y}$	measured fluxes, labels and pool sizes
$\mathbf{M}_{\mathbf{w}}, \mathbf{M}_{\mathbf{y}}, \mathbf{M}_{\mathbf{Y}}$	measurement matrices for fluxes, labels and pool sizes
$\varepsilon_{\mathbf{w}}, \varepsilon_{\mathbf{y}}, \varepsilon_{\mathbf{Y}}$	measurement noise vectors for fluxes, labels and pool sizes

1 Introduction

1.1 Stationary Flux Analysis

The detailed quantitative knowledge of intracellular metabolic fluxes in vivo is of fundamental importance for the study of microbial metabolism and metabolic engineering, which means an engineering approach for the genetic improvement of metabolic processes with respect to desired products [Bai91, SS93, KA93]. In particular the knowledge of stationary intracellular fluxes in vivo is of immediate practical use for

- the verification of enzyme activities and bidirectional reaction steps taking place in vivo,
- the characterization of different physiological states [VS93, Jor95, SSdG+95], in order to achieve an empirical quantitative comparison of regulatory mechanisms,
- the detailed quantitative discrimination between genetically manipulated microorganisms,
- systematic control analysis using methods of metabolic control theory [Kac88, KW86, AW92].

1.2 Two Well-Established Methods

Stationary flux analysis aims at the quantitation of all intracellular fluxes in central metabolism when the microbial system is in a well defined balanced steady state. In the last years the metabolite balancing approach has become popular in the bioprocess engineering community [VS93, GFJA93, vHHH+94, Jor95]. It is based on direct measurements of the fluxes between the cells and the surrounding medium (henceforth called the *extracellular fluxes*).

On the other hand metabolic tracer experiments have long been used for stationary intracellular flux determination mostly in biochemical research [WHK+82, CSKW83, WK84, MSJ88]. This technique relies on the fractional isotopic enrichment within intracellular metabolites (henceforth called *fractional labeling*) that can be accessed with NMR or mass spectroscopy.

Both methods, the metabolite balancing approach as well as the tracer approach, expose some insufficiencies that cannot be overcome with one method alone. While it turned out that some rather unsafe assumptions on energy balancing have to be made for a complete flux analysis based on extracellular fluxes, only relative fluxes can be determined when solely labeling data is available. For this reason tracer studies have always been supported by a few directly available flux measurements but only recently several new developments in reaction engineering led to a tight integration of both approaches [STM+94, ZS95, MdGW+95]. Currently the tracer technique in combination with direct extracellular flux measurements is supposed to be the most powerful method for obtaining intracellular flux information with only a few modeling assumptions on the living system.

The focus of this contribution will be on tracer experiments in combination with the NMR measurement technique since bioprocess engineers are usually rather unfamiliar with these techniques. The reader is referred to [Hof86, VS93, VP94a] for more details on metabolite balancing. Throughout the text main emphasis will be on modeling and data analysis. The introduced mathematical tools will then be used for investigating the general potential of labeling experiments for getting information about the living system. Only those properties of NMR are discussed that are required for understanding the origin of the data sets used for flux analysis. More details on in vivo NMR can be taken from [Gad82, Mat82, Lon88, LHHV90] while recent developments in reaction engineering for in vivo NMR are reviewed in [WdG95]. An illustrative

application example concerned with the whole central metabolism of *Corynebacterium glutamicum* will conclude the text. The biological implications of the presented results are discussed in [MdGW+95, EdG95].

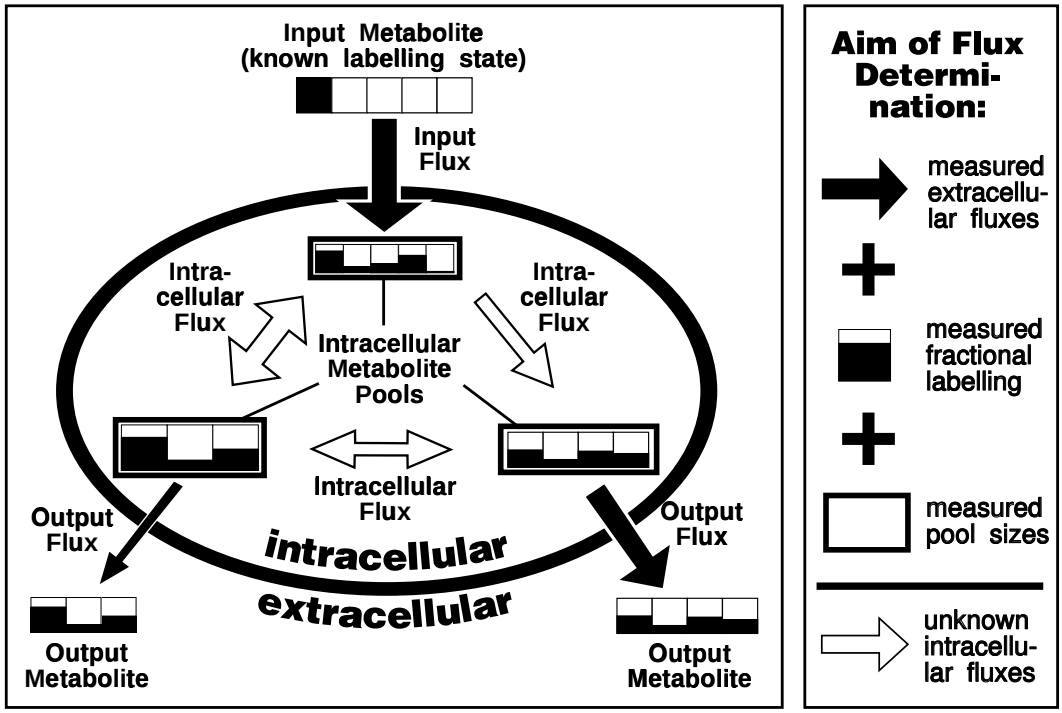

Figure 1: Available measurement data for stationary flux analysis: Extracellular fluxes, fractional carbon labeling, metabolite pool sizes

1.3 Data Sources for Stationary Flux Analysis

Reliable physiological data can only be obtained by measuring methods that do not influence the living system. The most familiar source of information is given by all quantitatively relevant extracellular fluxes like substrate consumption, product formation, biomass growth or gas efflux. These fluxes can easily be obtained from standard bioreactor instrumentation [Sch91] and analytical procedures using simple mass balancing.

The other source of data is presented by the isotopic label distribution in intermediates and products obtained from tracer experiments. Briefly, a metabolic carbon isotope tracer experiment is carried out by replacing a substrate (e.g. glucose) with a substrate that is ^{13}C or ^{14}C labeled at a certain carbon atom position. From this moment on, the label is distributed over the whole network until finally, the fractional labeling in all carbon atoms of intracellular metabolites equilibrates. In other words after running through an *isotopically instationary* state the system finally reaches an *isotopically stationary* state but always remains in a *metabolically stationary* state.

It depends on the experimental setup and the measurement technique whether the isotopically instationary state can be observed or only the final isotopically stationary state. Fig. 8 in [WdG95] illustrates the dynamic progress of an isotopically instationary ^{13}C tracer experiment with respect to labeling as observed within an NMR instrument while Table 2 in this contribution is based on stationary data.

Carbon tracer experiments are the most often used isotope labeling experiments for quantitative flux determination although ^{2}H and ^{15}N tracers or tracer combinations have also been

applied [KWR88, RCRL90, Lon92, MBW94, RKBY94]. Among the carbon isotopes ^{13}C has become the most popular because it can be easily detected with an NMR instrument. For this reason we concentrate here on ^{13}C labeling.

Evaluating isotopically instationary tracer experiments requires the additional knowledge of intracellular metabolite pool sizes. In some cases these can already be derived from additional NMR measurements or otherwise they have to be measured from cell extracts (cf. [WdG95]). If both data sources are not available it may be possible to estimate the pool sizes as well as the unknown fluxes from the measured data by parameter-fitting (see section 4.7).

1.4 Some Typical Experimental Setups

The resulting data set for flux quantitation is illustrated in Fig. 1. If it is sufficiently large, all intracellular fluxes can be quantitated based on very few assumptions on the living system as will be shown below. Some basic types of experiments for achieving this goal can now be distinguished where in many cases the experiment has been repeated with differently labelled input substrates [SB79, RB85, CB83]:

1. only extracellular fluxes are measured [VS93, GFJA93, Jor95].
2. only labeling fractions in an isotopically stable state are measured [WHK$^+$82, WK84, SEdGS93]
3. extracellular flux measurements are combined with labeling fractions from an isotopically stationary state [SB79, JWBL89, STM$^+$94, ZS95, MdGW$^+$95],
4. extracellular flux measurements and the time course of label enrichment in an isotopically instationary state is observed [KKW79, FHBS90, WGKF$^+$92, CFGC95]
5. extracellular flux measurements and so called isotopomer fractions (see section 1.6) in an isotopically stationary state are available [MSJ88, KWL93, KCS93, DRM$^+$93]

1.5 Preconditions for Stationary Flux Analysis

As mentioned before, stationary flux determination by tracer experiments combined with extracellular flux measurements relies on only a few modeling assumptions. However these should be explicitly mentioned:

1. The system is in a metabolic stationary state during the time span taken by the experiment. Clearly, this can be established inside a modern controlled bioreactor operated in a continuous culture mode (e.g. in turbidostatic or nutristatic culture).
2. For the metabolic pathways of interest, all reaction steps of the underlying biochemical network must be known with respect to the involved biochemical reactions and the fate of all carbon atoms within each step. For the central metabolism this knowledge is well established and can be taken from any biochemistry text book.
3. It is assumed that enzymes make no difference between labeled and unlabeled species of their substrates. Of course this is the basic assumption for all kinds of tracer studies. However, it should be mentioned that some small molecules have been shown to expose isotope mass effects under certain conditions [Wol82, O'L82, WKKS82].

4. The measurement process does not influence the cell function. This holds true for standard online instruments and modern sampling techniques with rapid cell inactivation if only small samples are taken [WdG95]. On the other hand, although it is generally assumed that strong magnetic fields do not affect microbial metabolism this is questioned by a recent publication [Oku94]. However using the measurement procedure of [Mar94] the organisms are actually not cultivated inside the NMR instrument so that this assumption is no more required (cf. section 2.4).

5. In the case where analysis of cellular material is performed after the experiment (e.g. from cell extracts or whole inactivated cells) it must be assured that the measured data is representative for the in vivo state of the system (cf. section 2.4).

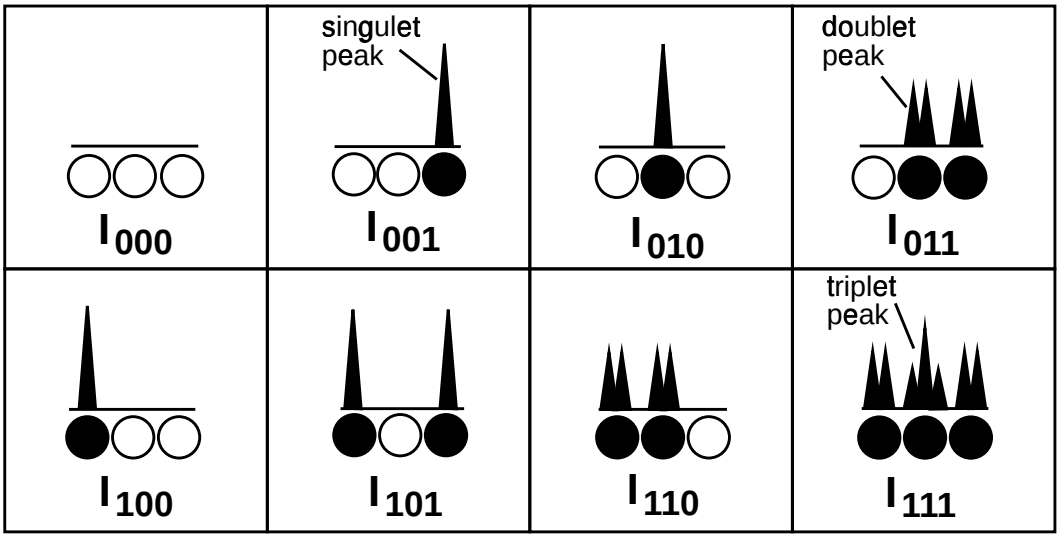

Figure 2: The $2^3 = 8$ different ^{13}C-isotopomers of an ideal molecule I with 3 carbon atoms. White circles correspond to ^{12}C, black circles to ^{13}C. When identical scalar coupling constants between adjacent carbon atoms are assumed (ideal case) the peak patterns in the corresponding high resolution NMR spectra are schematically shown.

1.6 Isotopomers

Up to now it is not clear, why ^{13}C labeling has outgrown the classical ^{14}C technique in the last years. The reason is that — apart from the intrinsic problems of working with radioactive material — much more information can be obtained much easier by using the NMR technique. This will be explained now in some more detail (cf. [Lon88, JRMS91]).

The main problem of tracer quantitation is to distinguish between labeled carbon atoms at different positions within one metabolite. To this end in classical carbon isotope approaches the metabolites had to be extracted and chemically degraded for separating the single carbon atom positions [SB79, CRSK81, DRM$^+$93]. In contrary to this time-consuming procedure an NMR instrument allows to directly localize all ^{13}C labeled atoms at the same time within a mixture of substances. This is even possible within intact cells using in vivo NMR (cf. [WdG95]).

Even more information can be obtained with an NMR instrument because so called isotopomers can — at least in part — be distinguished. The isotopomers of a metabolite with n carbon atoms represent the 2^n possible labeling states in which this molecule can be encountered

(Fig. 2). It will turn out in section 1.8 that in fact more information about intracellular fluxes can be obtained from isotopomer data than from positional carbon labeling data alone.

Clearly, isotopomer measurement is beyond the reach of classical methods based on chemical treatment. Only mass spectroscopy is also capable of distinguishing between isotopomers. Applications to flux determination are described in [IL87, DRM+93, KWL93]. However, mass spectrometry can only distinguish between those isotopomers with different numbers of labeled carbon atoms while more isotopomer fractions can be quantitated with NMR (cf. 4.6 and Fig. 2).

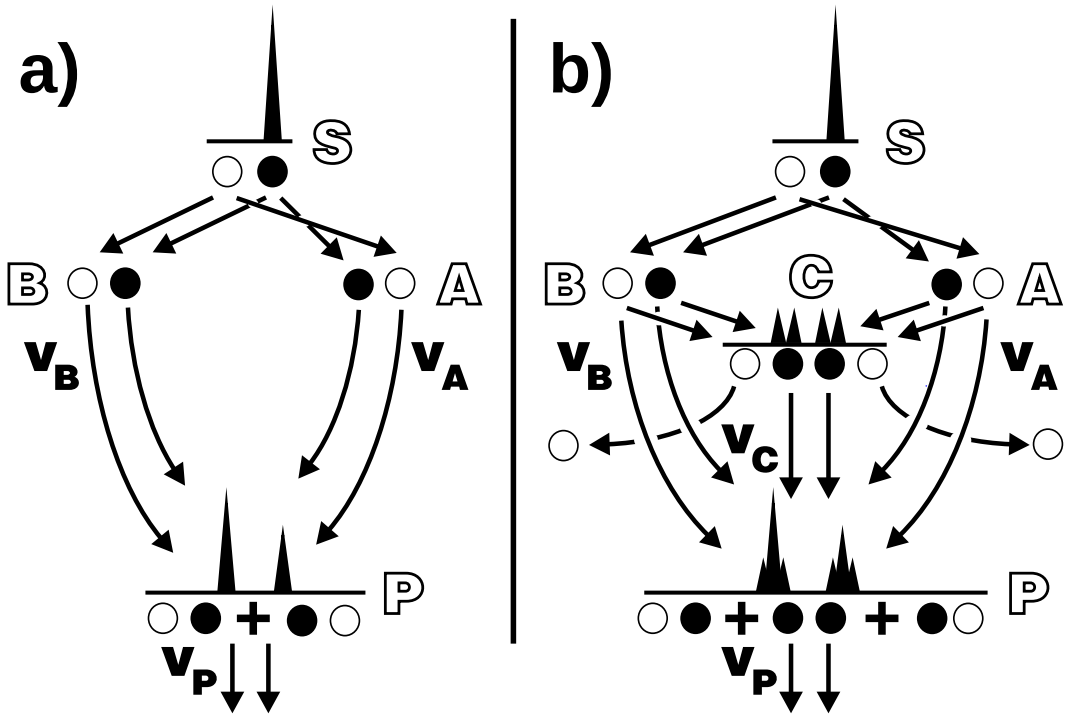

Figure 3: Example networks demonstrating the superiority of tracer experiments for flux determination compared to methods based on extracellular fluxes alone. a) Two alternate pathways for producing P can be distinguished based on positional carbon labels. b) Three pathways can be distinguished based on isotopomers by multiplet measurement.

1.7 The Significance of Fractional Carbon Labeling Data

Clearly, extracellular flux data is directly related to intracellular fluxes by stoichiometric balance equations. On the other hand it is not clear a priori that labeling data contains any information on fluxes. A very simple example shown in Fig. 3a makes clear that there are indeed strong relations between fluxes and fractional labels even in isotopic equilibrium.

The example shows a network with two alternate parallel pathways for the formation of a product P from a substrate S both with two carbon atoms. The alternate pathways via the intracellular metabolites A and B are distinguished by the different fate of the carbon atoms from S. If a [2-^{13}C]-labeled substrate is fed into the system (see Fig. 3a) two different isotopomers of the product will emerge, one labeled at the first and the other at the second carbon position.

Assume now that the fluxes in the alternate pathways are given by v_A, v_B and the percentage of labeling for both carbon atoms of P are given by p_1, p_2. From this we get:

$$\frac{v_A}{v_B} = \frac{p_1}{p_2}$$

Consequently the flux ratio can be determined from the label fraction ratio. A similar situation is encountered within *Corynebacterium glutamicum* which produces lysine using two different pathways [SSK+91]. The above argument was used in [SEdGS93] to quantitate the usage of these different pathways (see also [WK84]).

Clearly this information cannot be calculated from any direct extracellular flux measurement. On the other hand the example reveals the general property of tracer experiments that without (absolute) extracellular flux measurements only flux ratios can be computed. If in the example the product formation $v_P = v_A + v_B$ is known in addition we get (notice that $p_1 + p_2 = 1$ because labeling is conserved in the system)

$$v_A = p_1 \cdot v_P \qquad v_B = p_2 \cdot v_P$$

Of course there would be no measurable effect if the fate of the label would be the same in both branches. As a rule of thumb the flux information that can be obtained from labeling experiments heavily depends on the extent to which position-changing of carbon atoms occurs. Fortunately, it happens quite frequently that labeled carbon atoms are distributed over the complete metabolic network. This finally explains why carbon tracers are the most promising isotopes for intracellular flux determination while e.g. ^{15}N can only be used for special investigations [KWR88].

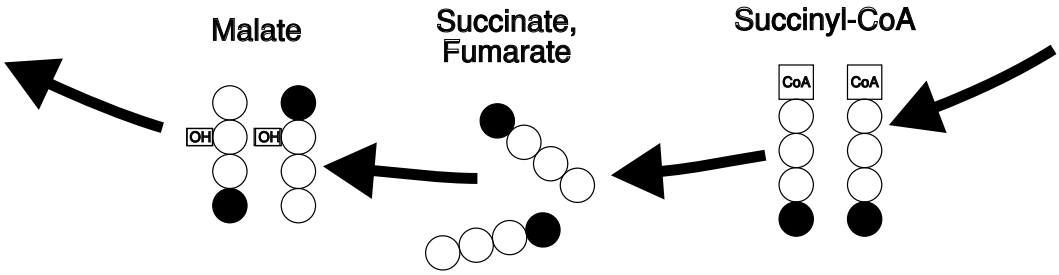

Figure 4: Label scrambling in the citric acid pathway. The symmetric molecules of succinate and fumarate can freely change their orientation so that labeled carbon atoms finally occur in two positions of malate with equal probability.

1.8 The Significance of Fractional Isotopomer Data

The example can be further extended for demonstrating that isotopomer measurements can reveal even more details about flux distributions. In Fig. 3b another product formation step has been added that produces P from A and B via a bimolecular reaction step. With the indicated [2-^{13}C] substrate labeling this reaction forms a third isotopomer of P with both positions labeled.

The additional flux is denoted by v_C and the isotopomer percentages in P are given as indicated in Fig. 3b by p_{01}, p_{11}, p_{10} (note that the unlabeled isotopomer does not occur). We then have $p_{01} + p_{10} + p_{11} = 1$ and $v_P = v_A + v_B + v_C$ so that:

$$v_A = p_{10} \cdot v_P \qquad v_B = p_{01} \cdot v_P \qquad v_C = p_{11} \cdot v_P$$

Of course this result cannot be produced with positional carbon atom labeling measurements alone. On the other hand the carbon labeling state can be reconstructed from the isotopomer knowledge as

$$p_1 = p_{10} + p_{11} \qquad p_2 = p_{01} + p_{11}$$

and thus the example demonstrates that isotopomer analysis is always superior or at least equipotent to positional carbon label analysis (cf. section 5.4).

Clearly, the presence of a bimolecular reaction step is essential for producing this effect. A similar situation is encountered in the citric acid cycle where carbon atoms can change positions within scrambling reactions (Fig. 4). This basically is the phenomenon that is used in [MSJ88, Lee93] for quantifying citric acid fluxes from isotopomer measurements.

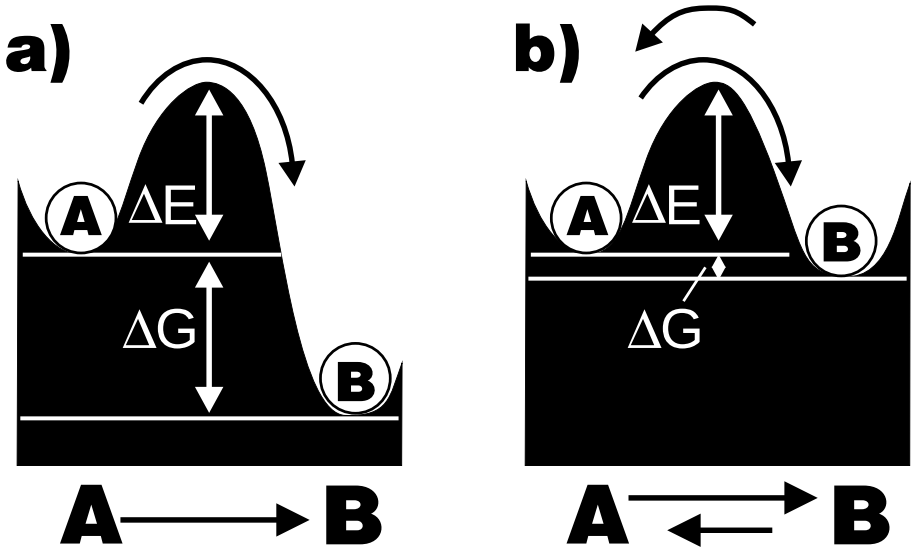

Figure 5: Uni- and bidirectional reaction steps from the thermodynamic viewpoint. It depends on the in vivo free reaction energy ΔG and the activation energy ΔE whether a reaction proceeds in only one direction or in both directions simultaneously.

1.9 Relations between Stationary and Kinetic Modeling

A short comparison between stationary flux analysis and the investigation of the dynamic behaviour of metabolic fluxes in response to changing extracellular conditions shall conclude this section. Both approaches strongly differ with respect to the experimental procedures and measurement equipment used as well as the results that can be achieved. On the other hand their common goal is to obtain a quantitative characterization of biochemical reaction steps in vivo. In both situations very recently a number of powerful new experimental techniques has been developed (cf. [WdG95]).

With respect to mathematical modeling, dynamic investigations always aim at the development and experimental validation of detailed kinetic models of intracellular metabolism (e.g. [DLC$^+$84, WBA92]). On the other hand, for the metabolically stationary situation models are required to compute unknown intracellular fluxes from stationary measurement data. There are some interrelations between the stationary and the dynamical approach showing that both are really complementary to each other:

- Usually kinetic models approximate the dynamics of metabolism around a certain stationary state [SV91, WBA92]. Consequently, stationary analysis supplies the cornerstones for dynamic modeling.

- No assumptions on kinetic mechanisms have to be made for stationary modeling. Consequently, the results of stationary flux determination are expected to be more reliable than those from mechanistic modeling.

- As will be shown in section 4.4 a distinguishing feature of stationary tracer experiments is their potential for quantifying both directions of a bidirectional reaction step under certain conditions [WdGA95] (Fig. 5). This may be a valuable information for distinguishing equilibrating reaction steps from controlling reaction steps in vivo. Moreover, for mechanistic modeling this has the consequence that reversible enzymatic mechanisms have to be taken into consideration [Seg75, MTBK89, WBA92].

- Of course, results from stationary flux analysis are only valid around the investigated metabolic state [VP94b]. On the other hand a validated mechanistic model may expose a larger prediction horizon and may even be capable of forecasting the effect of genetic modifications. However, in both cases a series of experiments under different conditions has to be performed in order to obtain a complete picture.

2 Measuring Stationary Intracellular Data

2.1 Extracellular Flux Data

Almost all stationary studies make use of extracellular flux measurements to a certain degree. If a bioreactor is used for cell cultivation the extracellular fluxes can be calculated using mass balancing from concentration measurements and the dilution rate. For example HPLC or FIA instruments, gas efflux measurements and the determination of biomass concentration can be used for this purpose (cf. [WdG95]).

An important idea was the incorporation of cell mass composition for the quantitation of the anabolic fluxes that use precursors from central metabolism [Hol86, Val91]. As shown by [NIS90] the biosynthetic pathways of any cell component can be uniquely traced back to 12 precursors in central metabolism. These are glucose-6-phosphate, fructose-6-phosphate, ribose-5-phosphate, erythrose-4-phosphate, glyceraldehyde-3-phosphate, 3-phosphoglycerate, phosphoenolpyruvate, pyruvate, acetyl-coenzyme A, α-ketoglutarate, succinyl-coenzyme A and oxaloacetate. From this knowledge, the knowledge of cell composition and the determined biomass growth rate a detailed quantitation of the corresponding 12 effluxes from central metabolism is obtained which dramatically improves the available information.

For convenience many experiments rely on the assumption that biomass composition in microorganisms is constant over a large variety of metabolic states and microorganisms [Roe83, Val91]. Of course this assumption deserves great care and ought to be experimentally verified from time to time though this is a very laborious task.

2.2 Some more Details on NMR Spectra

In order to understand the following modeling considerations some more details on NMR spectra are now briefly sketched at the risk of oversimplification. The reader is referred to [WdG95, Mat82, Gad82, Lon88, LHHV90] for an in depth discussion of in vivo NMR measurement techniques.

NMR spectra are superpositions of resonance spectra from all resonating atoms within the sample. In principle each ^{13}C atom produces a unique resonance peak in the NMR spectrum. Its frequency position depends on the electro-chemical surrounding of this atom in the metabolite it is part of. The area of the corresponding resonance peak is directly proportional to the concentration. An example spectrum taken from an in vivo experiment is given in Fig. 8 of [WdG95].

In most cases the ^{13}C isotopes are not directly observed but ^{1}H NMR is used instead as an indirect measuring technique. The ^{13}C isotopes then become detectable by a changed resonance

pattern of the surrounding protons since their ^{1}H peaks split up into peaks from ^{12}C-bound protons and peaks from ^{13}C-bound protons. This enables the relative amount of labeled carbon atoms to be determined without knowing the absolute amount of the examined substance. Due to the low chemical shift dispersion and broad complex multiplet structures ^{1}H spectra are much harder to interpret than ^{13}C spectra. For this reason metabolites usually have to be purified before they can be effectively measured with ^{1}H NMR [SEdGS93]. An example spectrum is given in Fig. 6.

The situation becomes even more difficult when high resolution spectra are taken for detecting isotopomers. The underlying phenomenon is that — due to scalar spin-spin-coupling — a ^{13}C resonance peak corresponding to some carbon atom splits up into a so called multiplet peak when adjacent atoms are labeled too. The number of peaks in the multiplet depends on the number of labeled neighbours so that doublets, triplets, quartets and so on can be observed. It depends on the specific molecule which spectra will actually result from isotopomers. Fig. 2 schematically shows for an ideal C-3 body how in principle the spectral peaks correspond to certain labeling states of the observed molecules while Fig. 7 shows what comes out for a real metabolite (glutamate). However the exact correspondence between isotopomers and spectra in most cases is known in advance from published NMR data (e.g. [BD85]).

It becomes clear now, why ^{13}C does not always allow to completely separate between all possible isotopomers (compare to [KCS93, JSJ^{+}93, DRM^{+}93]). For example in Fig. 2 a mixture of the isotopomers I_{100} and I_{001} will produce singulet peaks on the first and third position from which both isotopomer fractions can be quantitated. On the other hand if I_{101} is also present in the mixture the two peaks cannot been uniquely attributed to the three isotopomers (cf. section 4.6).

Figure 6: Proton NMR spectra of ^{13}C labeled glutamate extracted from protein of *C. glutamicum* after incubation with [1-^{13}C]glucose. Lower trace: ^{13}C-decoupled spectrum showing a) H-2, b) H-3, c) H-4 protons of glutamate and d) signals from impurities. Upper trace: corresponding ^{13}C satellite position signals obtained after subtracting the ^{13}C-decoupled spectrum from the ”normal” proton spectrum as explained in [SEdGS93].

Figure 7: ^{13}C isotopomer spectra of the ^{13}C labeled glutamate shown in Fig. 6. Multiplets are due to scalar coupling with adjacent ^{13}C atoms (cf. [KCS93])

2.3 Approaches for NMR of Biological Samples

In vivo NMR techniques are reviewed in [WdG95] so that only the most important facts are summarized here. The principal problem associated with NMR of biological samples is its low sensitivity compared to other techniques like mass spectroscopy. The quality of an NMR signal depends on the measurement duration for producing the spectrum and the amount of labeled material within the sample. For isotopomer quantitation, high resolution spectra are required while a lower resolution may be sufficient for determining only positional carbon enrichment. If the isotopically instationary state has to be observed the measurement duration for one spectrum is strongly limited resulting in generally low signal to noise ratios. These problems have been partly overcome in the last years by the development of more powerful NMR instruments, the increased availability of ^{13}C labeled substrates and the experimental techniques that are described in the following.

The strongest in vivo NMR signals are obtained when the volume of the NMR receiver coil is completely occupied by cellular material as is approximately the case in many studies on perfused organs [MSJ88, DRM$^+$93]. In this situation ^{13}C NMR spectra with acceptable signal to noise ratio can be produced in less than a minute for metabolites in the milimolar concentration range. This allows time courses [CFGC95] and even isotopomers to be observed [MSJ88, KCS93].

In contrast to mammalian organs, microorganisms expose much higher oxygen demands and faster growth rates. As a consequence even in hollow fiber bioreactors well suited for high density cultivation of mammalian cells they cannot be maintained in such high concentrations and in a well defined reproducible and stable physiological state (cf. [WdG95]). One way to overcome these problems was to take concentrated cell suspensions [WHK$^+$82, WK84, dHUB$^+$86].

However it is doubtful if such results are representative for the in vivo state.

The best systems presently available for in vivo NMR studies of microorganisms under truly well defined stationary conditions in continuous culture are specially developed continuous flow NMR bioreactors [dGWP+92, Har95]. In such reactors cell densities of up to 30-50 g/l (dry cell mass) can be maintained and measured on line with in vivo NMR. These systems are very well suited for monitoring time courses of ^{13}C label incorporation [WdG95]. On the other hand the obtained spectral quality is still not optimal for isotopomer determination.

When mixtures of labeled substances are measured — as is always the case with whole cells — a great many signals of different compounds in widely differing concentrations can be found in the spectrum. In particular for low resolution spectra the peaks may significantly overlap [SB88]. This poses the problem of spectral deconvolution for disentangling the resonances and computing the peak areas. Several numerical methods have been developed to treat this problem [DAM88, NS89, MTG94, WMWdG95].

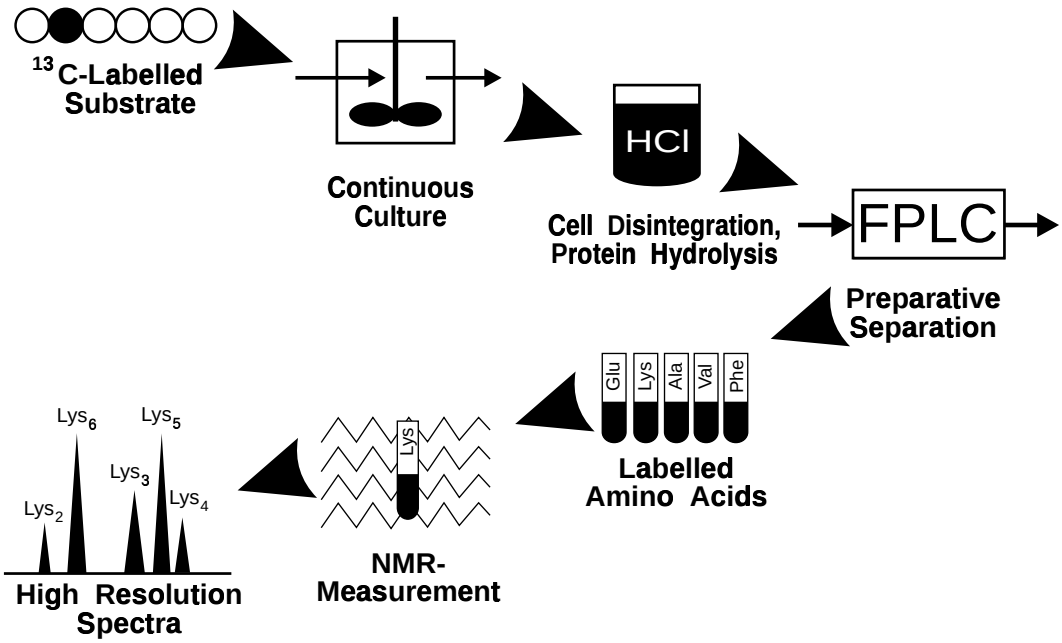

Figure 8: Decoupling production of labeled material from measuring by protein hydrolization after cultivation. Amino acid fractions are obtained by preparative separation methods.

2.4 Decoupling Production of Labeled Material from Measuring

An important idea for improving the NMR signal quality was to decouple the biological labeling experiment from the NMR measuring process. Taking samples and extracting intracellular metabolites is in general not sufficient because most substances are far too low concentrated (usually below 1 mmol) to produce an NMR signal. A successful approach is to take advantage of the cells own anabolism, i.e. of the fact that most intermediates are finally stored in cellular components like protein, lipids, RNA or DNA. In this form they are hidden from NMR observation but can be extracted by hydrolization in combination with preparative analytic measures (Fig. 8). Several authors report the extraction of glycerol from lipids [ESS83, CB83, RB85], ribonucleotides from RNA/DNA [ESS83, ESW+93] and amino acids from protein [ESS83, SEBF92, Mar94, PWK94].

The obtained fractions can be kept in the NMR instrument for an arbitrarily long time so that high resolution spectra and even multiplet peaks can be observed [SEBF92]. It is a great advan-

tage of the stationary approach that no absolute pool concentrations are required (cf. section 4.7) and mass deficiencies occurring during the separation process do not change the labeling fractions in the sample. On the other hand the isotopically instationary states cannot be reconstructed with this technique.

Clearly, the largest amount of quantitative information can be taken from the amino acids because they are synthesized from precursors at many different positions in the central metabolic network. From their labelling state the fractional enrichment of their pecursors can be immediately derived. Most of these precursor pools are inaccessible with other methods because they are too lowly concentrated in vivo. This technique has firstly been used in a quantitative manner in [MdGW$^+$95] which at the same time is the first application of the tracer technique to a continuously cultivated microorganism.

As pointed out in section 1.5 it must be assured that the measured data is representative for the in vivo state of the system. In particular the isotopically steady state of the system has to be guaranteed [BS82, ESW$^+$93]. This is a nontrivial problem since at the time when the intermediary metabolic pools have reached an isotopicically stationary state after switching to the labeled substrate this still does not hold for the cell components. The reason is that the cell mass in the bioreactor is originally unlabeled. However, after several cell residence times unlabeled cell material is washed out until finally the fractional labeling in the cell protein is representative for the in vivo state. On the other hand only a limited number n of residence times can be awaited for financial reasons, which can be corrected by the *washout correction factor* [MdGW$^+$95]

$$\text{WCF} \stackrel{def}{=} \frac{1}{1 - e^{-n}} \,. \tag{1}$$

3 Modeling of Metabolic ^{13}C Labeling Systems

3.1 Modeling Frameworks for Tracer Experiments

In order to evaluate the data sets from ^{13}C labeling experiments a model has to be formulated that quantitatively describes the relations between fluxes and ^{13}C labels. This model can then be fitted to the measured extracellular fluxes and intracellular fractional labels.

Carbon isotope labeling studies fall within the general category of tracer experiments. General models and mathematical tools for tracer analysis have already been developed in the seventies; an excellent textbook is [And83]. However there are some new aspects in metabolic carbon isotope labeling systems compared to general linear tracer systems:

- In "classical" applications of tracer experiments the model contains only a few pools (usually less than 10) and only one or two of them could be observed [LR83]. This is compensated by the availability of isotopically instationary observations (i.e. time courses). In the case of metabolic systems the situation is frequently quite different because a larger number of pools can be observed but only in the isotopically stationary state.

- Each metabolic reaction step induces several carbon atom transitions that take place with the same reaction rate. This allows to impose further constraints on metabolic tracer systems that are not given in the general case.

- The intracellular labeling state can be independently influenced by the forward and backward flux of a bidirectional reaction step (see section 4.4). Although this effect is well known for general tracer systems [And83, LR83] it has seldom been taken into account

for metabolic networks in large extent [SB79, CB83, KC83, CFGC95]. Thus, bidirectional steps should be conceptionally integrated into a general modeling framework [SSH92, WdGA95].

- Isotopomer dynamics cannot be handled within the framework of linear tracer kinetics because quadratic equations are required to describe the system (see section 3.11). On the other hand they still expose some general structure that can be formalized using a concise matrix notation from [Wie95c].

In the context of network modeling and data evaluation it is advisable to set up a general modeling framework for studying arbitrary nets and to facilitate variational studies. A so called structural system representation using matrix notation for separating network properties from flux and label variables greatly facilitates the development of general mathematical tools for simulation and system analysis [Red88, Wie95b]. However, only in a few cases a general structural modeling approach has been taken [HS93, ZS94, MdGW$^+$95]. The modeling framework presented below is based on the general linear tracer model [And83, BS82] while general modeling of exchange rates is done as in [MdGW$^+$95] and basic equations for isotopomer balancing taken from [Wie95c].

3.2 Constructing the Biochemical Network

Constructing a model for labeling systems requires the knowledge of all biochemical reaction steps in the network under consideration and moreover the fate of all carbon atoms within each reaction step. A simple formal notation first introduced in [WdG93] is used here to represent this information. It is derived from the familiar chemical sum notation presented in [VS93] and can be later used for automatic model generation. As an example the transaldolase step in the pentose phosphate pathway is written as:

$$\begin{array}{lccccccc} \mathrm{TA:} & \mathrm{GAP} & + & \mathrm{S7P} & > & \mathrm{E4P} & + & \mathrm{F6P} \\ & \#\mathrm{ABC} & + & \#\mathrm{abcdefg} & > & \#\mathrm{defg} & + & \#\mathrm{abcABC} \end{array}$$

This means that the first carbon atom of GAP (denoted by the sign # and the capital letter A) is taken over to the fourth carbon atom of F6P and so on.

Some bimolecular reaction steps require consideration of two molecules of one substance. This is conveniently expressed by including this substance two times and denoting the duplicate carbon atoms with different symbols. E.g. the conversion of fructose 1,6-bisphosphate to glyceraldehyde 3-phosphate is simply written as

$$\begin{array}{lccccc} \mathrm{ALD:} & \mathrm{F16BP} & > & \mathrm{GAP} & + & \mathrm{GAP} \\ & \#\mathrm{ABCDEF} & > & \#\mathrm{CBA} & + & \#\mathrm{DEF} \end{array}$$

Scrambling reactions (Fig. 4) are usually assumed to be symmetric, i.e. both scrambling steps have equal probability. Thus the situation shown in Fig. 4 can be easily expressed by:

$$\begin{array}{lccccccc} \mathrm{SCR:} & \mathrm{SUCCCOA} & + & \mathrm{SUCCCOA} & > & \mathrm{MAL} & + & \mathrm{MAL} \\ & \#\mathrm{ABCD} & + & \#\mathrm{UVWX} & > & \#\mathrm{ABCD} & + & \#\mathrm{XWVU} \end{array} .$$

3.3 Noninteger Stoichiometric Coefficients

Sometimes non-integer coefficients have been used to represent further knowledge on metabolic networks [Roe83, VS93]. The most important example is biomass composition that can be represented by a biomass formation “reaction”. However, such equations make no sense when carbon atoms have to be traced through the network. Fortunately, they can be replaced by a set

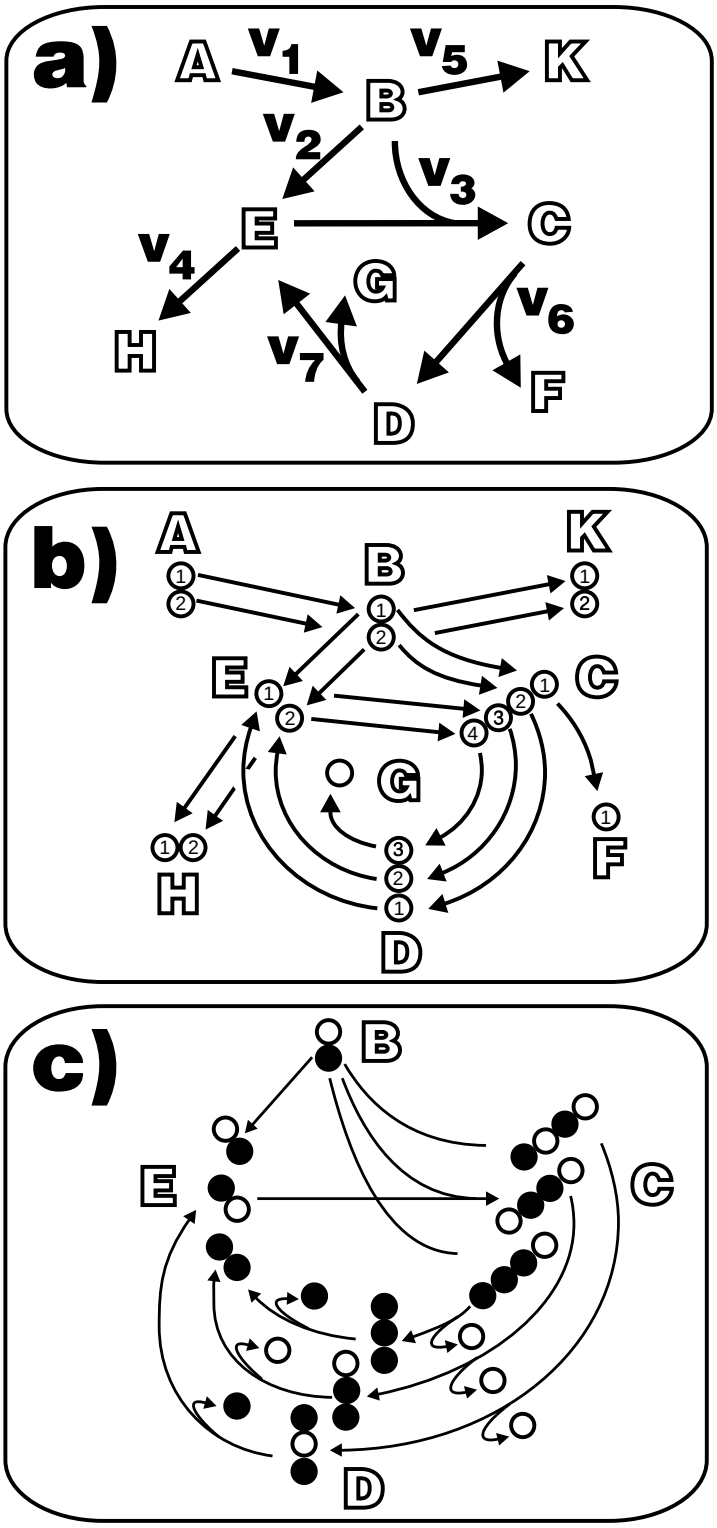

Figure 9: An example for demonstrating metabolite, carbon labeling and isotopomer balancing. a) metabolite network, b) carbon atom network, c) isotopomer network under the assumption that all steps are unidirectional and the input is labeled as indicated. In this situation only 13 of the 48 possible isotopomers are really produced.

of equations that describe the incorporation of each singular precursor metabolite into biomass. E.g. incorporation of glucose 6-phosphate into biomass is written as

$$\begin{array}{lllll} \mathrm{G6PBM:} & \mathrm{G6P} & > & \mathrm{G6PBiomass} \\ & \#\mathrm{ABCDEF} & > & \#\mathrm{ABCDEF} \end{array}$$

The corresponding "non-integer coefficient" is then supplied separately as a flux measurement value for $\mathrm{G6PBM}$ computed from biomass composition and growth rate. This is in any case the more natural way to account for biomass composition.

When no labeling data is available the measured carbon fluxes are usually not sufficient for determining the unknown intracellular fluxes from the stoichiometric balance equations. In this situation further assumptions have to be made [Val91], or other types of balances have to be considered in addition. As an example of an additional assumption some enzymes like the malic enzyme have been assumed inactive in [Val91]. On the other hand flux balancing is extended by considering energy metabolism (i.e. ATP, NADH or NADPH) in [Roe83, VS93, GFJA93, Jor95].

Usually the production of ATP from NADH is assumed as a reaction step with known stoichiometry. However, it should be noticed that oxidative phosphorylation is not based on a mechanism with fixed stoichiometry and only few things are known on its thermodynamic efficiency in vivo [Roe83, WvD87]. Moreover the possibility of futile cycling makes NADH, NADHP and ATP balancing a delicate problem [CF80, dHBS81, RB85, Pat92, CL94, CMCM+94]. The same holds for direct energy balancing based on free reaction energies [Roe83] which may heavily depend on the physiological situation, i.e. ΔG^0 values cannot be directly taken over to the in vivo situation (cf. [Mav93] and Fig. 5).

3.4 An Example System

In the following a simple example system taken from [Wie95c] is used for introducing the various balances that have to be formulated. It is chosen to demonstrate several general features of labeling systems with as few metabolites as possible. The reaction steps and carbon atom transitions in the system are given in the introduced formal notation by:

$$\begin{array}{llllllllll} \mathrm{v1:} & \mathrm{A} & & & > & \mathrm{B} & \quad \mathrm{v5:} & \mathrm{B} & > & \mathrm{K} \\ & \#12 & & & > & \#12 & & \#12 & > & \#12 \\ \mathrm{v2:} & \mathrm{B} & & & > & \mathrm{E} & \quad \mathrm{v6:} & \mathrm{C} & > & \mathrm{D} + \mathrm{F} \\ & \#12 & & & > & \#12 & & \#1234 & > & \#234 + \#1 \\ \mathrm{v3:} & \mathrm{B} & + & \mathrm{E} & > & \mathrm{C} & \quad \mathrm{v7:} & \mathrm{D} & > & \mathrm{E} + \mathrm{G} \\ & \#12 & + & \#34 & > & \#1234 & & \#123 & > & \#12 + \#3 \\ \mathrm{v4:} & \mathrm{E} & & & > & \mathrm{H} \\ & \#12 & & & > & \#12 \end{array}$$

Three networks are associated to this system [Wie94b]. The metabolite network is shown in Fig. 9a, the carbon network in Fig. 9b and a small section of the isotopomer network in Fig. 9c. It becomes clear that even for small systems isotopomer networks can become quite complex. For this reason a "full sized" section from central metabolism is completely unsuitable as an example.

However, the example network bears resemblance to the citric acid cycle in connection with the anaplerotic reaction section. It should be noticed that carbon atoms change their position after one turn in the citric acid cycle while they remain unchanged within an anaplerotic step. These properties are exposed by the example network too but much fewer carbon atoms are required.

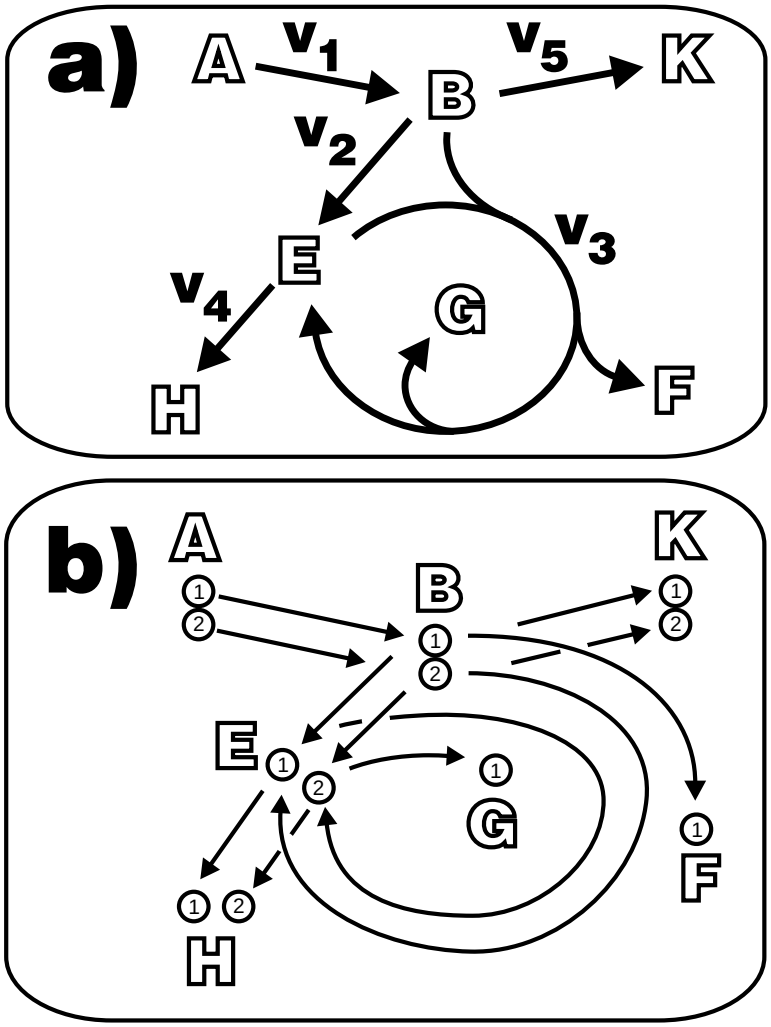

Figure 10: Reduced network from Fig. 9 as a result of network simplification: a) metabolite network, b) carbon atom network

3.5 Simplification of the Example System

To further reduce the number of isotopomers in the example system it is transformed now to an equivalent simpler system shown in Fig. 10. The idea behind this simplification is to backtrack the product carbon atoms $\mathrm{F}\#1$ and $\mathrm{G}\#1$ through the system. Obviously, it makes no difference if these atoms are already split off from $\mathrm{B}\#1$ and $\mathrm{E}\#2$ instead of $\mathrm{C}\#1$ and $\mathrm{D}\#3$. This allows to remove $\mathrm{C}\#1$, $\mathrm{D}\#3$ and $\mathrm{C}\#4$ from the system. Finally, G and C can be completely removed because nothing splits off at these stages. The remaining network now is composed from $\mathrm{v}1$, $\mathrm{v}2$, $\mathrm{v}4$, $\mathrm{v}5$ and the changed reaction step

$$\begin{array}{lccccccccc} \mathrm{v}3: & \mathrm{B} & + & \mathrm{E} & > & \mathrm{E} & + & \mathrm{F} & + & \mathrm{G} \\ & \#12 & + & \#34 & > & \#23 & + & \#1 & + & \#4 \end{array}$$

Although this network looks strange, all quantities related with the original network shown in Fig. 9 can be reconstructed from the following computations based on the reduced system. This emphasizes that network reduction is an important task whenever isotopomers have to be accounted for. The considerations made above give some impression of the typical simplification operations used in literature to reduce network complexity.

3.6 Flux State Variables

In the following the values of the metabolic fluxes $\mathrm{v}1$,...,$\mathrm{v}5$ are denoted by corresponding variables $v_i \geq 0$. More precisely, two variables $v_i^{\rightarrow}, v_i^{\leftarrow}$ have to be introduced representing each forward and backward flux direction (Fig. 5). Clearly, if a reaction step is irreversible, one of these fluxes is zero. In the example it will be assumed that the uptake and product formation steps $\mathrm{v}1$, $\mathrm{v}4$ and $\mathrm{v}5$ are irreversible (a familiar modeling assumption) as well as the intracellular step $\mathrm{v}3$. On the other hand $\mathrm{v}2$ is assumed to take place in both directions.

In order to comprise the forward and backward directions of all molar fluxes in the reaction network the vectors

$$\mathbf{v}^{\rightarrow} = \left(\, v_1^{\rightarrow}, v_2^{\rightarrow}, v_3^{\rightarrow}, v_4^{\rightarrow}, v_5^{\rightarrow} \, \right) \qquad \text{and} \qquad \mathbf{v}^{\leftarrow} = \left(\, v_1^{\leftarrow}, v_2^{\leftarrow}, v_3^{\leftarrow}, v_4^{\leftarrow}, v_5^{\leftarrow} \, \right)$$

(of equal dimension) are introduced. The additional irreversibility assumptions are given by

$$v_1^{\leftarrow} = v_3^{\leftarrow} = v_4^{\leftarrow} = v_5^{\leftarrow} = 0 \; .$$

The physical unit of fluxes is strictly taken to be [mol/h]. The reason is that a chemical reaction step does not only take over substrates to products but also substrate carbon atoms (respectively isotopomers) to product carbon atoms (respectively isotopomers). Clearly, if the unit [mol/h] is chosen, the same flux values $v_i^{\rightarrow}, v_i^{\leftarrow}$ can serve for representing metabolite fluxes as well as carbon or isotopomer fluxes.

Finally, from the vectors $\mathbf{v}^{\leftarrow}, \mathbf{v}^{\rightarrow}$ the composite overall flux vector

$$\mathbf{v} = \begin{pmatrix} \mathbf{v}^{\rightarrow} \\ \mathbf{v}^{\leftarrow} \end{pmatrix}$$

(of twice the dimension) and the corresponding net flux vector

$$\mathbf{v}^{\mathrm{net}} = \mathbf{v}^{\rightarrow} - \mathbf{v}^{\leftarrow}$$

is formed (notice that with standard measurement equipment only some of these net fluxes can be observed). Clearly, all components of $\mathbf{v}$ must be nonnegative which is expressed by the componentwise inequality

$$\mathbf{v} \geq \mathbf{0} \; .$$

3.7 Pool State Variables

The labeling state is always represented by the percentage of labeled material at all carbon atom positions. Only the intermediary metabolites and the metabolites fed into the system have to be accounted for balancing. For denoting the label fractions within a metabolite like B small indexed letters b_1, b_2 are used. In general all intermediary carbon atom pools under consideration have to be enumerated. This gives rise to the fractional label variables $\mathbf{x}_i \in [0,1]$ and the overall labeling vector $\mathbf{x}$. In our case only B and E are intermediates such that

$$\mathbf{x} = (b_1, b_2, e_1, e_2)^T \ .$$

A special type of carbon atoms are those that fed into the system as a metabolic substrate because their labeling state is known a priori. These atoms are enumerated likewise and comprised to the constant input labeling vector

$$\mathbf{x}^{\text{inp}} = (a_1, a_2)^T \ .$$

When isotopomers are considered the situation is much more complex. We distinguish between the isotopomer fractions of one metabolite by using a binary number that specifies, which carbon atoms are labeled [FR95]. For instance the $2^2 = 4$ isotopomer fractions of B are denoted by $b_{00}, b_{01}, b_{10}, b_{11}$. Since carbon atoms and isotopomers cannot be confused in the following the symbol $\mathbf{x}$ is used again to denote the isotopomer fraction state vector

$$\mathbf{x} = (b_{00}, b_{01}, b_{10}, b_{11}, e_{00}, e_{01}, e_{10}, e_{11})^T \tag{2}$$

and the relations

$$\begin{array}{lll} b_{00}{+}b_{01}{+}b_{10}{+}b_{11}{=}\ 1 & b_{10}{+}b_{11}{=}\ b_1 & e_{10}{+}e_{11}{=}\ e_1 \\ e_{00}{+}e_{01}{+}e_{10}{+}e_{11}{=}\ 1 & b_{01}{+}b_{11}{=}\ b_2 & e_{01}{+}e_{11}{=}\ e_2 \end{array} \tag{3}$$

always hold between isotopomer and carbon label fractions. As in the carbon atom case, the vector $\mathbf{x}^{\text{inp}}$ of input isotopomers has to be defined as:

$$\mathbf{x}^{\text{inp}} = (a_{00}, a_{01}, a_{10}, a_{11})^T$$

Finally, the modeling of isotopically instationary experiments requires the knowledge of absolute molar pool sizes. For a specific metabolite they are denoted by capital italic letters like B for the pool size of B. In the general model the corresponding pool variables are comprised to the vector

$$\mathbf{X} = (B, E) \ .$$

3.8 Metabolite Balance Equations

Several types of material balances can now be formulated for each intracellular pool using the introduced state variables. The first is the well known stoichiometric balance equation [Hof86] that holds for the fluxes participating in one metabolite pool. Because the absolute pool sizes do not change in a metabolic stationary state the sums of incoming and outgoing fluxes must be equal. In the example the stoichiometric balance equations corresponding to the intermediary metabolite pools are:

$$\begin{array}{lrcl} B: & v_1^{\rightarrow} + v_2^{\leftarrow} & = & v_2^{\rightarrow} + v_3^{\rightarrow} + v_5^{\rightarrow} \\ E: & v_2^{\rightarrow} + v_3^{\rightarrow} & = & v_2^{\leftarrow} + v_3^{\rightarrow} + v_4^{\rightarrow} \end{array} \tag{4}$$

By introducing the stoichiometric matrix

$$\mathbf{N} = \begin{pmatrix} 1 & -1 & -1 & . & -1 \\ . & 1 & . & -1 & . \end{pmatrix}$$

this can be more conveniently expressed as

$$\mathbf{0} = \mathbf{N} \cdot \mathbf{v}^{\text{net}} \,. \tag{5}$$

3.9 Stationary Carbon Label Balance Equations

When carbon atom labeling is considered a carbon label balance can be written for each intermediary carbon pool. In this situation the above reaction system should be interpreted as a system of carbon atom transitions:

v1:	A#1	>	B#1	v3:	B#1	>	F#1	v4:	E#1	>	H#1
v1:	A#2	>	B#2	v3:	B#2	>	E#1	v4:	E#2	>	H#2
v2:	B#1	>	E#1	v3:	E#1	>	E#2	v5:	B#1	>	K#1
v2:	B#2	>	E#2	v3:	E#2	>	G#1	v5:	B#2	>	K#2

The carbon label balance for B#1 is constructed now as follows: The amount of labeled material that is carried over to B#1 by the incoming flux v1 from A#1 and the backward flux of v2 from E#1 is given by $v_1^{\rightarrow} \cdot a_1 + v_2^{\leftarrow} \cdot e_1$. On the other hand the outgoing fluxes v2, v3 and v5 take the amount of $(v_2^{\rightarrow} + v_3^{\rightarrow} + v_5^{\rightarrow}) \cdot b_1$ out of B#1. If the complete system is assumed to be in isotopically stationary state the following set of carbon label balance equations comes out:

$$\begin{array}{rrcrcl} b_1: & v_1^{\rightarrow}\cdot a_1 & + & v_2^{\leftarrow}\cdot e_1 & = & (v_2^{\rightarrow}+v_3^{\rightarrow}+v_5^{\rightarrow})\cdot b_1 \\ b_2: & v_1^{\rightarrow}\cdot a_2 & + & v_2^{\leftarrow}\cdot e_2 & = & (v_2^{\rightarrow}+v_3^{\rightarrow}+v_5^{\rightarrow})\cdot b_2 \\ e_1: & v_3^{\rightarrow}\cdot b_2 & + & v_2^{\rightarrow}\cdot b_1 & = & (v_2^{\leftarrow}+v_3^{\rightarrow}+v_4^{\rightarrow})\cdot e_1 \\ e_2: & v_3^{\rightarrow}\cdot e_1 & + & v_2^{\rightarrow}\cdot b_2 & = & (v_2^{\leftarrow}+v_3^{\rightarrow}+v_4^{\rightarrow})\cdot e_2 \end{array} \tag{6}$$

Again this can be more conveniently expressed using matrix notation as

$$\begin{pmatrix} 0 \\ 0 \\ 0 \\ 0 \end{pmatrix} = \begin{pmatrix} v_1^{\rightarrow} & . \\ . & v_1^{\rightarrow} \\ . & . \\ . & . \end{pmatrix} \cdot \begin{pmatrix} a_1 \\ a_2 \end{pmatrix}$$

$$+ \begin{pmatrix} -v_2^{\rightarrow} - v_3^{\rightarrow} - v_5^{\rightarrow} & . & v_2^{\leftarrow} & . \\ . & -v_2^{\rightarrow} - v_3^{\rightarrow} - v_5^{\rightarrow} & . & v_2^{\leftarrow} \\ v_2^{\rightarrow} & v_3^{\rightarrow} & -v_2^{\leftarrow} - v_3^{\rightarrow} - v_4^{\rightarrow} & . \\ . & v_2^{\rightarrow} & v_3^{\rightarrow} & -v_2^{\leftarrow} - v_3^{\rightarrow} - v_4^{\rightarrow} \end{pmatrix} \cdot \begin{pmatrix} b_1 \\ b_2 \\ e_1 \\ e_2 \end{pmatrix}$$

Here the input labels a_1, a_2 are separated from the intermediary labels. Clearly, this equation has the general structure

$$\mathbf{0} = \mathbf{P}^{\text{inp}}(\mathbf{v}) \cdot \mathbf{x}^{\text{inp}} + \mathbf{P}(\mathbf{v}) \cdot \mathbf{x} = (\sum_i \mathbf{v}_i \cdot \mathbf{P}_i^{\text{inp}}) \cdot \mathbf{x}^{\text{inp}} + (\sum_i \mathbf{v}_i \cdot \mathbf{P}_i) \cdot \mathbf{x} \tag{7}$$

where $\mathbf{P}_i, \mathbf{P}_i^{\text{inp}}$ are called the atom transition matrices [WdGA95] (compare to the closely related atom mapping matrices in [ZS94]). For example we have:

$$P_2^{\rightarrow} = \begin{pmatrix} -1 & . & . & . \\ . & -1 & . & . \\ 1 & . & . & . \\ . & 1 & . & . \end{pmatrix}, \quad P_2^{\leftarrow} = \begin{pmatrix} . & . & 1 & . \\ . & . & . & 1 \\ . & . & -1 & . \\ . & . & . & -1 \end{pmatrix}, \quad P_1^{\text{inp}} = \begin{pmatrix} 1 & . \\ . & 1 \\ . & . \\ . & . \end{pmatrix}$$

3.10 Instationary Carbon Label Balance Equations

If the system is not in isotopic equilibrium a differential equation system has to be formulated. In this situation the absolute pool sizes $\mathbf{X}_j$ play a role because they determine the capacity of a pool for labeled material. In the example the absolute amount of labeled material in the first position of B is given by $B \cdot b_1$ so that $d/dt\,(B \cdot b_1) = B \cdot d/dt\, b_1$ when the system is in a metabolic stationary state. This term has to be added to the label balance equation at stage $\mathrm{B}\#1$ in Eq. (6).

In order to get a general matrix representation similar to Eq. (7) a matrix $\mathbf{I}$ is constructed that enlarges the vector $\mathbf{X}$ to the dimension of $\mathbf{x}$ by appropriately repeating its entries. In the example:

$$\mathbf{I} \cdot \mathbf{X} \stackrel{def}{=} \begin{pmatrix} 1 & . \\ 1 & . \\ . & 1 \\ . & 1 \end{pmatrix} \begin{pmatrix} B \\ C \end{pmatrix} = \begin{pmatrix} B \\ B \\ C \\ C \end{pmatrix}$$

Putting all parts together we get the instationary balance equation system

$$\mathrm{diag}\,(\mathbf{I} \cdot \mathbf{X}) \cdot \frac{d}{dt}\,\mathbf{x} = \mathbf{P}^{\mathrm{inp}}\,(\mathbf{v}) \cdot \mathbf{x}^{\mathrm{inp}} + \mathbf{P}\,(\mathbf{v}) \cdot \mathbf{x} \tag{8}$$

where $\mathrm{diag}\,(\mathbf{I} \cdot \mathbf{X})$ is the diagonal matrix constructed from the vector $\mathbf{I} \cdot \mathbf{X}$.

3.11 Isotopomer Balance Equations

When isotopomers are considered the situation is more complicated because the number of educts involved in a reaction step determines the (algebraic) order of the reaction equation. In the example the reaction step $\mathrm{v}3$ has two substrates so that at the isotopomer level all reactions

$$\begin{array}{lllllllllll}
\mathrm{v}3: & \mathrm{B}\#00 & + & \mathrm{E}\#00 & > & \mathrm{E}\#00 & + & \mathrm{F}\#0 & + & \mathrm{G}\#0 \\
\mathrm{v}3: & \mathrm{B}\#00 & + & \mathrm{E}\#01 & > & \mathrm{E}\#00 & + & \mathrm{F}\#0 & + & \mathrm{G}\#1 \\
\mathrm{v}3: & \mathrm{B}\#00 & + & \mathrm{E}\#10 & > & \mathrm{E}\#01 & + & \mathrm{F}\#0 & + & \mathrm{G}\#0 \\
\mathrm{v}3: & \mathrm{B}\#00 & + & \mathrm{E}\#11 & > & \mathrm{E}\#01 & + & \mathrm{F}\#0 & + & \mathrm{G}\#1 \\
\mathrm{v}3: & \mathrm{B}\#01 & + & \mathrm{E}\#00 & > & \mathrm{E}\#10 & + & \mathrm{F}\#0 & + & \mathrm{G}\#0 \\
\mathrm{v}3: & \mathrm{B}\#01 & + & \mathrm{E}\#01 & > & \mathrm{E}\#10 & + & \mathrm{F}\#0 & + & \mathrm{G}\#1 \\
\mathrm{v}3: & \mathrm{B}\#01 & + & \mathrm{E}\#10 & > & \mathrm{E}\#11 & + & \mathrm{F}\#0 & + & \mathrm{G}\#0 \\
\mathrm{v}3: & \mathrm{B}\#01 & + & \mathrm{E}\#11 & > & \mathrm{E}\#11 & + & \mathrm{F}\#0 & + & \mathrm{G}\#1 \\
\mathrm{v}3: & \mathrm{B}\#10 & + & \mathrm{E}\#00 & > & \mathrm{E}\#00 & + & \mathrm{F}\#1 & + & \mathrm{G}\#0 \\
\mathrm{v}3: & \mathrm{B}\#10 & + & \mathrm{E}\#01 & > & \mathrm{E}\#00 & + & \mathrm{F}\#1 & + & \mathrm{G}\#1 \\
\mathrm{v}3: & \mathrm{B}\#10 & + & \mathrm{E}\#10 & > & \mathrm{E}\#01 & + & \mathrm{F}\#1 & + & \mathrm{G}\#0 \\
\mathrm{v}3: & \mathrm{B}\#10 & + & \mathrm{E}\#11 & > & \mathrm{E}\#01 & + & \mathrm{F}\#1 & + & \mathrm{G}\#1 \\
\mathrm{v}3: & \mathrm{B}\#11 & + & \mathrm{E}\#00 & > & \mathrm{E}\#10 & + & \mathrm{F}\#1 & + & \mathrm{G}\#0 \\
\mathrm{v}3: & \mathrm{B}\#11 & + & \mathrm{E}\#01 & > & \mathrm{E}\#10 & + & \mathrm{F}\#1 & + & \mathrm{G}\#1 \\
\mathrm{v}3: & \mathrm{B}\#11 & + & \mathrm{E}\#10 & > & \mathrm{E}\#11 & + & \mathrm{F}\#1 & + & \mathrm{G}\#0 \\
\mathrm{v}3: & \mathrm{B}\#11 & + & \mathrm{E}\#11 & > & \mathrm{E}\#11 & + & \mathrm{F}\#1 & + & \mathrm{G}\#1
\end{array}$$

may happen. Clearly, the probability of two isotopomers with fractional amounts b_i and b_j to meet in step $\mathrm{v}3$ is given by $b_i \cdot b_j$ [KCS93]. Consequently, the corresponding total isotopomer flux is $v_3^{\rightarrow} \cdot b_i \cdot b_j$. Thus isotopomer balancing for bimolecular steps leads to bilinear terms with respect to the $\mathbf{x}_i$ while for the monomolecular steps $\mathrm{v}1$, $\mathrm{v}2$, $\mathrm{v}4$ and $\mathrm{v}5$ and the effluxes from each pool all terms in the corresponding balance equations are exactly analogous to those in Eq. (7) respectively Eq. (8). The complete equation system then is:

$$
\begin{array}{lrcll}
b_{00}: & v_1^{\rightarrow}\cdot a_{00} & + & v_2^{\leftarrow}\cdot e_{00} & = (v_2^{\rightarrow}+v_3^{\rightarrow}+v_5^{\rightarrow})\cdot b_{00}\\
b_{01}: & v_1^{\rightarrow}\cdot a_{01} & + & v_2^{\leftarrow}\cdot e_{01} & = (v_3^{\rightarrow}+v_2^{\rightarrow}+v_5^{\rightarrow})\cdot b_{01}\\
b_{10}: & v_1^{\rightarrow}\cdot a_{10} & + & v_2^{\leftarrow}\cdot e_{10} & = (v_3^{\rightarrow}+v_2^{\rightarrow}+v_5^{\rightarrow})\cdot b_{10}\\
b_{11}: & v_1^{\rightarrow}\cdot a_{11} & + & v_2^{\leftarrow}\cdot e_{11} & = (v_3^{\rightarrow}+v_2^{\rightarrow}+v_5^{\rightarrow})\cdot b_{11}\\
e_{00}: & v_2^{\rightarrow}\cdot b_{00} & + & v_3^{\rightarrow}\cdot(b_{00}+b_{10})\cdot(e_{00}+e_{01}) & = (v_2^{\leftarrow}+v_3^{\rightarrow}+v_4^{\rightarrow})\cdot e_{00}\\
e_{01}: & v_2^{\rightarrow}\cdot b_{01} & + & v_3^{\rightarrow}\cdot(b_{00}+b_{10})\cdot(e_{10}+e_{11}) & = (v_2^{\leftarrow}+v_3^{\rightarrow}+v_4^{\rightarrow})\cdot e_{01}\\
e_{10}: & v_2^{\rightarrow}\cdot b_{10} & + & v_3^{\rightarrow}\cdot(b_{01}+b_{11})\cdot(e_{00}+e_{01}) & = (v_2^{\leftarrow}+v_3^{\rightarrow}+v_4^{\rightarrow})\cdot e_{10}\\
e_{11}: & v_2^{\rightarrow}\cdot b_{11} & + & v_3^{\rightarrow}\cdot(b_{01}+b_{11})\cdot(e_{10}+e_{11}) & = (v_2^{\leftarrow}+v_3^{\rightarrow}+v_4^{\rightarrow})\cdot e_{11}
\end{array}
$$

Again a comprehensive matrix notation is desirable. Clearly, the linear terms in $\mathbf{x}$ can still be expressed with the matrix notation introduced in Eq. (7). On the other hand the bilinear terms in $\mathbf{x}$ are represented by introducing one symmetric matrix for each balance equation. For example the e_{11} step can be written as follows:

$$
\begin{aligned}
e_{11}: 0 = \frac{1}{2}\cdot v_3^{\rightarrow}\cdot
&\begin{pmatrix} b_{00}\\ b_{01}\\ b_{10}\\ b_{11}\\ e_{00}\\ e_{01}\\ e_{10}\\ e_{11}\end{pmatrix}^T
\cdot
\begin{pmatrix}
. & . & . & . & . & . & . & . \\
. & . & . & . & . & . & 1 & 1 \\
. & . & . & . & . & . & . & . \\
. & . & . & . & . & . & 1 & 1 \\
. & . & . & . & . & . & . & . \\
. & . & . & . & . & . & . & . \\
. & 1 & . & 1 & . & . & . & . \\
. & 1 & . & 1 & . & . & . & .
\end{pmatrix}
\cdot
\begin{pmatrix} b_{00}\\ b_{01}\\ b_{10}\\ b_{11}\\ e_{00}\\ e_{01}\\ e_{10}\\ e_{11}\end{pmatrix}
\quad
\begin{array}{l} + \quad v_2^{\rightarrow} \quad \cdot b_{11}\\ -(v_2^{\leftarrow}+v_3^{\rightarrow}+v_4^{\rightarrow})\cdot e_{11}\end{array}
\end{aligned}
$$

The symmetric matrix in this equation will be denoted by $\mathbf{Q}_{3,11}^{\rightarrow}$ indicating the flux number and the target pool. All such matrices $\mathbf{Q}_{i,j}$ corresponding to the same flux variable $\mathbf{v}_i$ can then be composed to a 3-dimensional matrix structure (i.e. a tensor) $\mathbf{Q}_i$ (which may be thought of as a vector of square matrices) and a 3D-matrix-times-vector product can then be defined as

$$
\mathbf{x}^T\cdot\mathbf{Q}_i\cdot\mathbf{x} = \mathbf{x}^T\cdot\begin{pmatrix}\mathbf{Q}_{i,1}\\ \mathbf{Q}_{i,2}\\ \vdots\\ \mathbf{Q}_{i,n}\end{pmatrix}\cdot\mathbf{x} \stackrel{def}{=} \begin{pmatrix}\mathbf{x}^T\cdot\mathbf{Q}_{i,1}\cdot\mathbf{x}\\ \mathbf{x}^T\cdot\mathbf{Q}_{i,2}\cdot\mathbf{x}\\ \vdots\\ \mathbf{x}^T\cdot\mathbf{Q}_{i,n}\cdot\mathbf{x}\end{pmatrix}.
$$

Using this notation the isotopomer balance equations can finally be written quite similar to Eq. (7) as [Wie95c]:

$$
\begin{aligned}
\mathbf{0} &= \mathbf{P}^{\text{inp}}(\mathbf{v})\cdot\mathbf{x}^{\text{inp}} + \mathbf{P}(\mathbf{v})\cdot\mathbf{x} + \mathbf{x}^T\cdot\mathbf{Q}(\mathbf{v})\cdot\mathbf{x}\\
&= (\sum_i \mathbf{v}_i\cdot\mathbf{P}_i^{\text{inp}})\cdot\mathbf{x}^{\text{inp}} + (\sum_i \mathbf{v}_i\cdot\mathbf{P}_i)\cdot\mathbf{x} + \mathbf{x}^T\cdot(\sum_i \mathbf{v}_i\cdot\mathbf{Q}_i)\cdot\mathbf{x} \qquad (9)
\end{aligned}
$$

Input 3D-matrices analogous to $\mathbf{P}^{\text{inp}}$ are not required because it can be assumed without loss of generality that any substrate enters the system via a monomolecular uptake step. It should be clear now how in principle reactions with more than two substrates can be represented. However, since such reaction steps can in practice be replaced by successive bimolecular reactions it is not necessary to introduce matrices with dimension higher than three. Finally, the instationary state equations are constructed completely analogous to Eq. (8).

Interestingly, isotopomers have always been considered in connection with the citric acid cycle [CSKW83, KWL93, KCS93, FR95] where essentially only one bimolecular step occurs

at the entry point of acetyl-coenzyme A. Since the labelling state of the input isotopomer is known the equations for the citrate cycle can be essentially written without any truly bilinear term (i.e. $\mathbf{Q}_i = 0$ for all i). This reduces the equation system to a linear model with respect to $\mathbf{x}$ which can be mathematically treated with the same methods as the ordinary carbon labelling system in Eq. 7 [CSKW83].

4 Simulation and Data Analysis

4.1 Network Synthesis

As shown above all model equations required for describing the isotope and isotopomer labeling system can be built up from certain vectors and matrices. However, the dimensions can become quite large. When the whole central metabolism including glycolysis, pentose phosphate pathway, citric acid cycle, glyoxylate shunt and anaplerotic reaction section is included the metabolic network has about 25 metabolite fluxes between 20 metabolite pools, 120 carbon fluxes between 80 carbon atom pools and 3.200 isotopomer fluxes between 600 isotopomer pools [Sch95, CFGC95]. This makes clear that computer aided tools for network synthesis and consistency checking are absolutely necessary. In particular model variation studies would be quite time-consuming when using manual input.

Most authors used highly specific programs for simulation or data analysis [CB83, JRMS91, KCS93] or general systems based on explicit equation input [WGKF$^+$92, Lee93]. Only a few general tools for carbon or isotopomer network synthesis have been designed based on explicit matrix input to generate the system equations [ZS94, HSG$^+$93]. However, for large systems network synthesis from either matrix or balance equation input is still not satisfying while for isotopomer systems this effort is almost prohibitive (cf. [CSKW83]).

A more convenient way for network synthesis is to write a compiler program for translating a minimal formal input like that presented in section 3.2 into the corresponding matrix structures. For metabolite flux networks several such programs are known [MSS90, Val91, Hof93] while for carbon atom and isotopomer networks the program NMRFlux described in [Wie94a] is currently the only implementation. The corresponding algorithms for isotopomer network synthesis are described in [Sch95]. Clearly, the input for other matrix- or equation-based simulation or computer algebra systems can be easily generated once a matrix representation is available [Wie94a].

An important feature of a network synthesis program is its ability to check formal consistency conditions. In [Wie94b] some criteria have been given that lead to consistent networks. In most cases it is sufficient to check the following criteria for detecting typing errors in the textual input: i) Any carbon atom of an educt must appear exactly once on the product side and vice versa, ii) each molecule must have the same number of carbon atoms within each equation, iii) input and output metabolites always occur in a monomolecular reaction.

4.2 Simulation

Simulation of ^{13}C labeling experiments means to predict the outcome of an experiment when all fluxes $\mathbf{v}$ are known. For this purpose values for the components $\mathbf{v}_i$ must be given in a way that the constraints imposed by the stoichiometric equations are respected. Usually the user of a simulation program wishes to fix certain values while others are varied in each simulation run. This process can be supported by appropriate software tools [Wie94a].

Assume now that a suitable vector $\mathbf{v} \geq \mathbf{0}$ is given. Simulation of ^{13}C labeling experiments then can proceed in different ways:

1. For isotopically instationary experiments the ordinary differential equations (8) associated to carbon or isotopomer fluxes have to be solved. For non-stiff systems a higher order Runge-Kutta scheme is well suited [HNW87]. On the other hand when highly reversing reactions occur the differential equation system will tend to become stiff. Specialized solvers [CSKW83, HW91], the preliminary introduction of rapid equilibria by pool lumping [SSH92] or the preliminary reduction of the network size [CB95] may solve these problems.

2. It is well known that linear tracer systems are globally stable except from some pathological situations because the corresponding system matrices $\mathbf{P}(\mathbf{v})$ are diagonally dominant [And83]. From this the negativity of all eigenvalues can be concluded. For the isotopomer equation system it can be likewise shown [Wie95c] that its linearization is diagonally dominant in any point $\mathbf{0} \leq \mathbf{x} \leq \mathbf{1}$. Such systems are called dissipative and can be proven to be globally stable too [MN91]. As a consequence the stationary state can always be computed using a differential equation solver as an iterative procedure.

3. Clearly, when only the stationary solution is of interest differential equation solving is inefficient because the transient states are of no interest. In particular the treatment of isotopomer systems can be time-consuming because of their high dimensionality. Modifying the well known Euler scheme by introducing relaxation leads to the iterative schemes for linear and nonlinear equation solving [BL94, Deu95]. In particular the Gauss-Seidel-Algorithm is used in [ZS94] for solving the linear carbon labeling balances and in [Sch95] to solve the isotopomer balances. In any situation the sparsity of the involved matrices can be exploited to speed up the computation.

4. In the case of carbon labeling systems equation (7) can be explicitly solved for the vector $\mathbf{x}$ because $\mathbf{P}(\mathbf{v})$ is invertible (which follows from its diagonal dominance) [BS82]:

$$\mathbf{x} \;=\; \mathbf{x}(\mathbf{v}) \;=\; -(\sum_i \mathbf{v}_i \cdot \mathbf{P}_i)^{-1}(\sum_i \mathbf{v}_i \cdot \mathbf{P}_i^{\text{inp}}) \cdot \mathbf{x}^{\text{inp}} \tag{10}$$

   It is well known that up to a dimension of about 100 the iterative solution of linear equation systems cannot compete with direct methods even when sparse matrix representations are used [Hac93]. This turned out to be true for labeling systems too [Sie95]. When a high numerical stability is required a QR factorization method accompanied by a preconditioner [Sie95] or an explicit monitoring of the condition number [FR95] is better suited.

4.3 Computing Explicit Solutions

In our example the stationary carbon labeling equations as well as the isotopomer equations can be solved explicitly using computer algebraic methods. For simplicity we henceforth assume that the input substrate is labeled at the second position, i.e.

$$a_1 = 0 \qquad a_2 = 1$$

or when expressed with isotopomers

$$a_{00} = 0 \qquad a_{01} = 1 \qquad a_{10} = 0 \qquad a_{11} = 0$$

To start with the calculation the stoichiometric equations (4) are used to eliminate the flux variables $v_3^{\rightarrow}$ and $v_4^{\rightarrow}$:

$$\begin{array}{rcl} v_3^{\rightarrow} & = & v_1^{\rightarrow} - v_2^{\rightarrow} + v_2^{\leftarrow} - v_5^{\rightarrow} \\ v_4^{\rightarrow} & = & v_2^{\rightarrow} - v_2^{\leftarrow} \end{array}$$

The resulting stationary carbon atom labeling fractions can then be obtained from Eq. (10) as:

$$\begin{array}{rcl} b_1 & = & v_2^{\leftarrow} \cdot \quad \alpha_1\alpha_2 \,/\, \alpha_0 \\ b_2 & = & \alpha_3 \,/\, \alpha_0 \\ e_1 & = & \alpha_1\alpha_2\alpha_4 \,/\, \alpha_0 \\ e_2 & = & \alpha_5 \,/\, \alpha_0 \end{array}$$

with the auxiliary terms α_i shown below.

For the isotopomer fractions the computation is much more difficult and in general impossible because the corresponding equation set is essentially nonlinear with respect to $\mathbf{x}$. However, in this special case the computer algebraic methods discussed in 5.3 help to compute the explicit result with the aid of a computer algebra system:

$$\begin{array}{rcl} b_{00} & = & 1 - b_{10} - b_{01} - b_{11} \\ b_{10} & = & v_2^{\rightarrow} v_2^{\leftarrow} \cdot \alpha_1\alpha_2\alpha_6 \,/\, \alpha_0^2 \\ b_{01} & = & \alpha_2\alpha_8 \,/\, \alpha_0^2 \\ b_{11} & = & v_2^{\leftarrow} \cdot \alpha_1^2\alpha_2^2\alpha_4 \,/\, \alpha_0^2 \end{array} \qquad \begin{array}{rcl} e_{00} & = & 1 - e_{10} - e_{01} - e_{11} \\ e_{10} & = & v_2^{\rightarrow} \cdot \alpha_1\alpha_2\alpha_4\alpha_6 \,/\, \alpha_0^2 \\ e_{01} & = & v_2^{\rightarrow} \cdot \quad \alpha_7 \,/\, \alpha_0^2 \\ e_{11} & = & \alpha_1^2\alpha_2^2\alpha_4^2 \,/\, \alpha_0^2 \end{array}$$

with

$$\begin{array}{rcl} \alpha_0 & = & v_1^{\rightarrow 3} \\ & & + v_1^{\rightarrow 2} \cdot (3v_2^{\leftarrow} - 2v_5^{\rightarrow}) \\ & & + v_1^{\rightarrow} \cdot (3v_2^{\leftarrow 2} - 4v_2^{\leftarrow} v_5^{\rightarrow} + v_5^{\rightarrow 2}) \\ & & + v_2^{\leftarrow} \cdot (v_2^{\leftarrow 2} - 2v_2^{\leftarrow} v_5^{\rightarrow} - v_2^{\rightarrow 2} + v_5^{\rightarrow 2}) \\ \alpha_1 & = & v_1^{\rightarrow} - v_2^{\rightarrow} + v_2^{\leftarrow} - v_5^{\rightarrow} \\ \alpha_2 & = & v_1^{\rightarrow} + v_2^{\leftarrow} - v_5^{\rightarrow} \\ \alpha_3 & = & \alpha_0 - v_2^{\rightarrow} v_2^{\leftarrow} \alpha_1 \end{array} \qquad \begin{array}{rcl} \alpha_4 & = & v_1^{\rightarrow} + v_2^{\leftarrow} \\ \alpha_5 & = & \alpha_0 - v_2^{\rightarrow} \alpha_1\alpha_4 \\ \alpha_6 & = & v_1^{\rightarrow 2} + v_1^{\rightarrow} \cdot (2v_2^{\leftarrow} - v_5^{\rightarrow}) \\ & & + v_2^{\leftarrow} \cdot (v_2^{\leftarrow} - v_2^{\rightarrow} - v_5^{\rightarrow}) \\ \alpha_7 & = & \alpha_0\alpha_6 + v_2^{\rightarrow} v_2^{\leftarrow} \cdot (2\alpha_6 v_2^{\rightarrow} - \alpha_0 - v_1^{\rightarrow} v_2^{\rightarrow 2}) \\ \alpha_8 & = & \alpha_7 - v_2^{\leftarrow} \alpha_1^3 \alpha_4 \end{array}$$

4.4 Explicit Flux Determination

Assume now that the flux values $v_1^{\rightarrow}$ and $v_5^{\rightarrow}$ can be directly measured and additionally the labels b_1, b_2 are available. Then the remaining unknown intracellular fluxes $v_2^{\rightarrow}, v_2^{\leftarrow}$ must be determined for reconstructing the whole system state. From the balance equations (6) the explicit solutions

$$\begin{array}{rcl} v_2^{\leftarrow} & = & v_1^{\rightarrow} \qquad\qquad \cdot \frac{b_1^2}{(b_2 - b_1)\cdot(b_2 + b_1 - 1)} \\ v_2^{\rightarrow} & = & (v_1^{\rightarrow} + v_2^{\leftarrow} - v_5^{\rightarrow}) \cdot \quad \frac{1 - b_2}{b_1} \end{array} \tag{11}$$

can be computed. The nonlinear mapping

$$\left(\frac{v_2^{\leftarrow}}{v_1^{\rightarrow}},\ \frac{v_2^{\rightarrow}}{v_1^{\rightarrow} + v_2^{\leftarrow} - v_5^{\rightarrow}} \right) \quad \overset{1-1}{\longleftrightarrow} \quad \left(\frac{b_1^2}{(b_2 - b_1)\cdot(b_2 + b_1 - 1)},\ \frac{1 - b_2}{b_1} \right)$$

thus can be used to visualize the correspondence between unknown fluxes and measured labels by a superposition of two contour plots (Fig. 11). A similar technique has been also used in [ZS94] as a graphical tool for flux estimation and sensitivity analysis.

An important observation can be taken from the example: Both directions of the reversible reaction step $\mathrm{v}2$ have been identified from labeling data. This proves once more that ^{13}C NMR labeling experiments are considerably more powerful that experiments that are solely based on metabolite balances. This observation motivates a more detailed consideration of bidirectional reaction steps in the next section.

It turns out that in the example situation isotopomer measurements are not necessary for flux determination. However, it is an interesting question, if this is still true, when the measurement $v_5^{\rightarrow}$ is no more available. In this situation the surplus values b_{11} and e_{01}, e_{10}, e_{11} may contain more information on the unknown fluxes. This question will be answered in section 5.4.

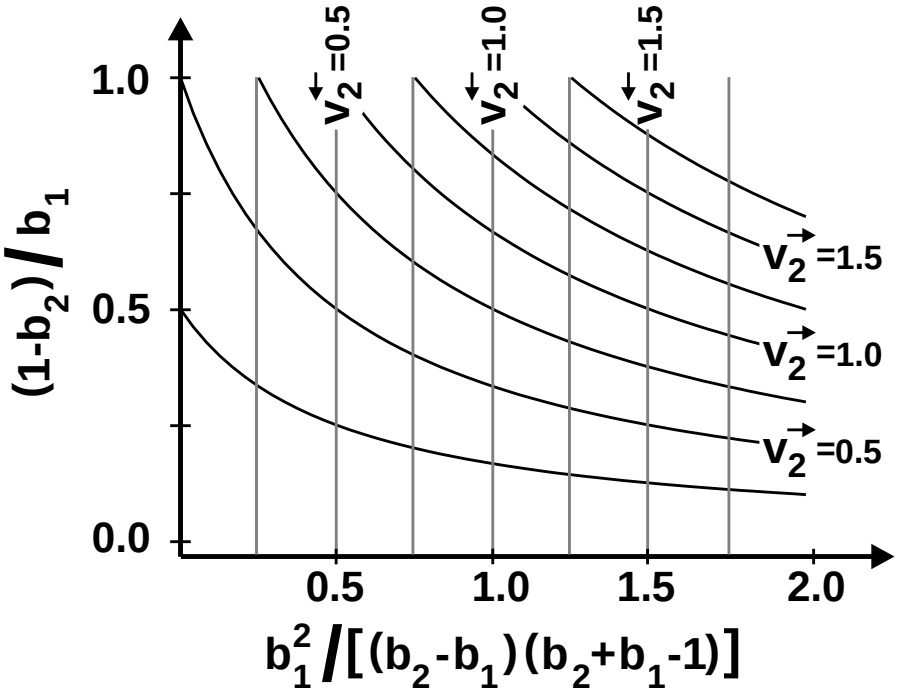

Figure 11: Superposition of two contour plots illustrating the computation of unknown intracellular fluxes from fractional labeling data. When two extracellular fluxes are assumed to be measured as $v_1^{\rightarrow} = 1.0$ and $v_5^{\rightarrow} = 0.5$ and measurements of b_1, b_2 are available the unknown fluxes $v_2^{\rightarrow}$ and $v_2^{\leftarrow}$ can be read off from the diagram.

4.5 Exchanging Reactions

When doing simulation studies on the influence of exchanging reactions it quickly becomes clear that forward and backward fluxes are well suited for formulating the balance equations (7) or (9) but rather inconvenient for expressing assumptions on exchange rates. To this end a more suitable coordinate system has to be found in which a forward/backward flux pair $\mathbf{v}_i^{\rightarrow}, \mathbf{v}_i^{\leftarrow}$ is described in terms of the net flux rate $\mathbf{v}_i^{\text{net}}$ and an appropriate exchange flux $\mathbf{v}_i^{\text{xch}}$. In [SSH92] the quantity $\mathbf{v}_i^{\text{xch}} = \mathbf{v}_i^{\rightarrow} + \mathbf{v}_i^{\leftarrow}$ is suggested for investigation of the system's behaviour when $\mathbf{v}_i^{\text{xch}} \rightarrow \infty$ (rapid equilibrium situation). However, this quantity is not convenient for describing irreversibility (i.e. $\mathbf{v}_i^{\rightarrow} = 0$ or $\mathbf{v}_i^{\rightarrow} = 0$) because it depends on $\mathbf{v}_i^{\text{net}}$ in this situation. Another definition from [MdGW$^+$95] that serves better for expressing irreversibility assumptions (but is rather inconvenient for analytical purposes) is given by (see also Fig. 12):

$$\mathbf{v}_i^{\text{xch}} = \min\left(\mathbf{v}_i^{\rightarrow}, \mathbf{v}_i^{\leftarrow}\right) \tag{12}$$

As can be easily verified that the pair $(\mathbf{v}_i^{\rightarrow}, \mathbf{v}_i^{\leftarrow})$ can be computed from $(\mathbf{v}_i^{\text{net}}, \mathbf{v}_i^{\text{xch}})$ and vice versa. Moreover it should be observed that $\mathbf{v}_i^{\text{xch}}$ is nonnegative but on the other hand it does not prescribe a certain net flux direction.

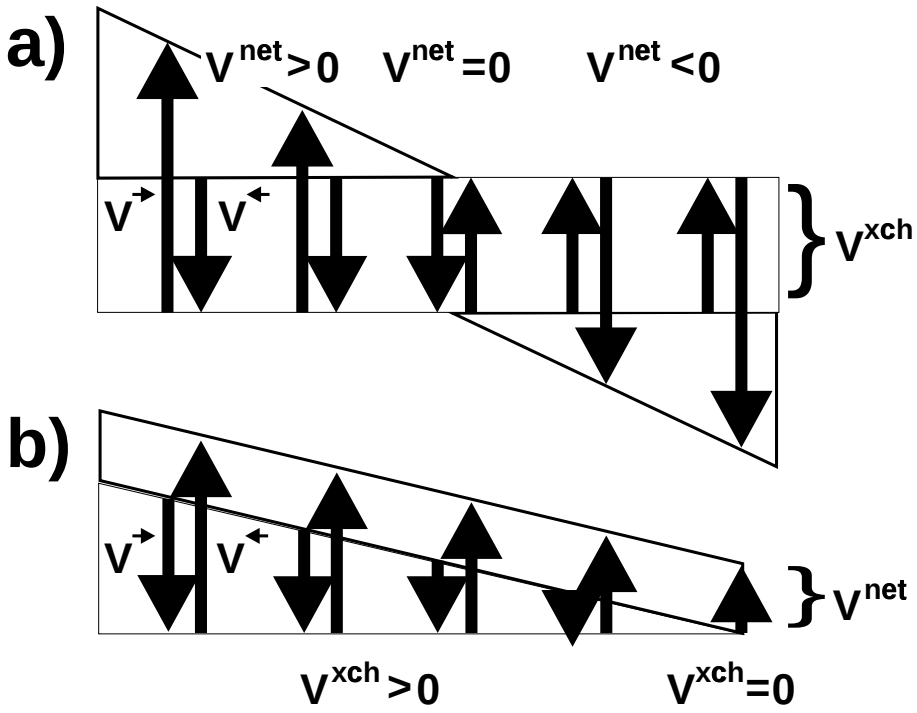

Figure 12: Definition of exchange fluxes for bidirectional reaction steps showing forward and backward flux for a) fixed exchange flux and varying net flux, b) fixed net flux and varying exchange flux.

Using $\mathbf{v}^{\text{xch}}$ physiological assumptions that are frequently made for biochemical reaction steps can be expressed as follows (cf. Fig. 5):

1. Irreversibility assumptions are usually made when large free energy differences are known from the in vitro situation (i.e. $\Delta G^0 \gg 0$). Moreover irreversibility must always be assumed for fluxes entering or leaving the system. Clearly, irreversibility of step i is expressed by $\mathbf{v}_i^{\text{xch}} = 0$.

2. Rapid equilibrium is the counterpart of irreversibility. In this case the forward and backward reaction takes place with a high rate compared to the net flux rate: $\mathbf{v}_i^{\text{xch}} \gg \mathbf{v}_i^{\text{net}}$.

3. Finally it is useful for simulation purposes to study the effect of a $\mathbf{v}_i^{\text{xch}}$-variation, by setting $\mathbf{v}_i^{\text{xch}}$ to arbitrary values.

A simulation run should be parametrized in the $(\mathbf{v}^{\text{net}}, \mathbf{v}^{\text{xch}})$ coordinate system where $\mathbf{v}^{\text{xch}}$ denotes the vector of all exchange fluxes. The stoichiometric equations and the assumptions made on the exchange fluxes impose linear constraints on these coordinates. The formal representation of these constraints can be easily handled by extending the stoichiometric equation (5) to a more general linear constraint equation:

$$\mathbf{N}^{\text{cnstr}} \cdot \begin{pmatrix} \mathbf{v}^{\text{net}} \\ \mathbf{v}^{\text{xch}} \end{pmatrix} = \mathbf{c}^{\text{cnstr}}$$

4.6 Measurement Equations

Incorporating measured values requires the introduction of measurement equations. Again a matrix notation is used where the measurement matrices $\mathbf{M}$ express which components of the state vectors have been measured. The vectors ε denote $N(\mathbf{0}, \mathbf{\Sigma})$-distributed noise terms with symmetric and positive definite covariance matrices $\mathbf{\Sigma}$. Usually the $\mathbf{\Sigma}$-matrices have diagonal shape, i.e. the measurements are assumed to be independent. With this notation we now get

$$\begin{array}{lrcl} \text{the flux measurement equation} & \mathbf{w} & = & \mathbf{M_w} \cdot \mathbf{v}^{\text{net}} + \varepsilon_{\mathbf{w}} \\ \text{the label or isotopomer measurement equation} & \mathbf{y} & = & \mathbf{M_y} \cdot \mathbf{x} \ + \varepsilon_{\mathbf{y}} \\ \text{the pool size measurement equation} & \mathbf{Y} & = & \mathbf{M_Y} \cdot \mathbf{X} \ + \varepsilon_{\mathbf{Y}} \end{array} \tag{13}$$

Clearly, the pool size measurement equation is only required in the isotopically instationary case. In this situation the label measurement equation must additionally be extended by a discrete time parameter.

When NMR multiplet analysis is used for isotopomer measurement, the isotopomer measurement matrix expresses how the measured values correspond to to the fractional amounts of isotopomers. In the example illustrated by figure 2 the observation is composed from singulet peaks s_1, s_2, s_3, doublet peaks d_1, d_2, d_3 and a triplet peak t_2. Moreover the sum of all percentages must be 1. The correspondence between these measured quantities and the isotopomer fractions is given by (cf. [KCS93, JSJ+93]):

$$\mathbf{M_y} \cdot x = \begin{pmatrix} 1 & 1 & 1 & 1 & 1 & 1 & 1 & 1 \\ . & . & . & . & 1 & 1 & . & . \\ . & . & 1 & . & . & . & . & . \\ . & 1 & . & . & . & 1 & . & . \\ . & . & . & . & . & . & 1 & 1 \\ . & . & . & 1 & . & . & 1 & . \\ . & . & . & 1 & . & . & . & 1 \\ . & . & . & . & . & . & . & 1 \end{pmatrix} \cdot \begin{pmatrix} i_{000} \\ i_{001} \\ i_{010} \\ i_{011} \\ i_{100} \\ i_{101} \\ i_{110} \\ i_{111} \end{pmatrix} = \begin{pmatrix} 1 \\ s_1 \\ s_2 \\ s_3 \\ d_1 \\ d_2 \\ d_3 \\ t_2 \end{pmatrix} = \mathbf{y}$$

Interestingly this $M_{\mathbf{x}}$ is not a full rank matrix but there remains only one degree of freedom do determine all isotopomer fractions from the measurements. Its kernel is generated by the vector $(1, -1, ., ., -1, 1, ., .)^T$, i.e. the isotopomers I#000,I#100,I#001 and I#101 cannot be separated (compare to section 2.2).

On the other hand if mass spectroscopy is used isotopomers can only be distinguished by their total mass so that measured quantities m_0, m_1, m_2, m_3 are obtained. We then have:

$$\begin{pmatrix} 1 & 1 & 1 & 1 & 1 & 1 & 1 & 1 \\ 1 & . & . & . & . & . & . & . \\ . & 1 & 1 & . & 1 & . & . & . \\ . & . & . & 1 & . & 1 & 1 & . \\ . & . & . & . & . & . & . & 1 \end{pmatrix} \cdot \begin{pmatrix} i_{000} \\ i_{001} \\ i_{010} \\ i_{011} \\ i_{100} \\ i_{101} \\ i_{110} \\ i_{111} \end{pmatrix} = \begin{pmatrix} 1 \\ m_0 \\ m_1 \\ m_2 \\ m_3 \end{pmatrix}$$

This is obviously much less information which explains why NMR is in principle superior to mass spectroscopy. However, both methods can be combined with the time-consuming chemical degradation technique which enables a complete isotopomer analysis to be performed [IL87, DRM+93].

4.7 Flux Estimation

In the general situation flux estimation cannot be achieved explicitly like in section 4.4 or graphically using the graphical superposition technique as demonstrated in Fig. 11 because the number of unknown parameters is too large for reasonably complex networks (cf. section 4.1). In this situation a nonlinear regression approach using the familiar least squares estimator is appropriate [BS82, SW89]. Knowing that $\mathbf{x}$ is always a function of $\mathbf{v}$ by Eq. (10) this flux estimate is obtained as the solution of the nonlinear programming problem:

$$\begin{array}{ll} \text{minimize} & \kappa(\mathbf{v}) = ||\mathbf{w} - \mathbf{M_v} \cdot \mathbf{v}^{\text{net}}||^2_{\mathbf{\Sigma_v}} + ||\mathbf{y} - \mathbf{M_x} \cdot \mathbf{x}(\mathbf{v})||^2_{\mathbf{\Sigma_x}} \\ \text{constrained by} & \mathbf{N}^{\text{cnstr}} \cdot \begin{pmatrix} \mathbf{v}^{\text{net}} \\ \mathbf{v}^{\text{xch}} \end{pmatrix} = \mathbf{c}^{\text{cnstr}} \\ \text{and} & \mathbf{v} \geq \mathbf{0} \end{array} \tag{14}$$

where $||\xi||^2_{\mathbf{\Sigma}} = \xi^T \cdot \mathbf{\Sigma}^{-1} \cdot \xi$ denotes the squared weighted norm corresponding to a covariance matrix $\mathbf{\Sigma}$. In the case where only flux measurements are available this is exactly the linear estimate for flux estimation from extracellular flux data proposed in [VS93] that can be directly computed using the Gauss-Markov theorem [Arn90].

In the isotopically instationary state the situation becomes more complex because usually not all pool sizes can be measured. Consequently, they have also to be estimated from the measured data, i.e. $\kappa(\mathbf{v})$ in Eq. (14) now becomes $\kappa(\mathbf{v}, \mathbf{X})$ and the sum of squares has to be extended by the term $||\mathbf{Y} - \mathbf{M_X} \cdot \mathbf{X}||^2_{\mathbf{\Sigma_X}}$.

This shows that instationary experiments require more information compared to the stationary case. This problem is usually treated by assuming fixed sizes for all small pools from literature data [FHBS90, WGKF+92, CFGC95] while taking measurements for the large pools [WGKF+92]. This strategy seems to be justified because the model outcoume is often very insensitive with respect to small pool sizes [WGKF+92, CFGC95].

4.8 Solution of the Flux Estimation Problem

In the majority of applications the flux estimation problem is solved explicitly as has been done in section 4.4. However this approach cannot in general make use of the complete measurement information. The same holds for the graphical approach (Fig. 11) that is strongly limited to dimensions one and two. On the other hand the general numerical solution of the flux estimation problem (14) poses several problems:

1. The linear constraints have to be resolved. This can be done with appropriate numerically stable matrix factorization techniques like singular value decomposition [PFTV88, Val91].

2. Exchange fluxes as defined by Eq. (12) are only piecewise differentiable functions. This problem can be treated with a derivative free algorithm like the well known Nelder Mead simplex algorithm at the cost of large computation times as has been done in [MdGW+95].

3. The inequality constraints $\mathbf{v} \geq \mathbf{0}$ have to be strictly obeyed. An ad hoc solution to overcome this problem is simply to replace $\mathbf{v}_i$ by some λ_i^2 which is always positive and then to minimize over λ_i. However, this will significantly decrease numerical stability.

4. While in older papers the minimimum of $\kappa(\mathbf{v})$ has been found manually by trial and error [KKW79, SB79] iterative optimization algorithms are now used [WGKF+92, KCS93, MdGW+95]. A modern successive quadratic programming algorithm that can simultaneously handle the constraints is developed in [Sie95].

5. In many cases the computational complexity of the instationary flux estimation problem has been overcome by more or less dramatical simplifications of the network [FHBS90, TDHW91, SSH92, CFGC95].

4.9 Statistical Analysis

Statistical analysis is required to judge the quality of the measured data and the obtained estimates. Several well established statistical methods can be applied for this purpose:

- The ability of the model to describe the measured data set can be tested [RB85, WGKF$^+$92, RDC$^+$95, FR95].
- Redundancies in the measured data set can be used to detect measurement errors [Val91, vHRH$^+$94, Wie95a].
- Sensitivity analysis of the model output with respect to the input parameters is used to study their influence [CB83, Lee93, CFGC95, CB95, Wie95b].
- The sensitivity of the estimated parameters with respect to the measured quantities show how the estimates are influenced by single measurements [Wie95b].
- The approximate covariance matrix for the estimated parameters can be computed and from this approximate parameter confidence regions can be constructed [RB85, KCS93, Wie95b].

All sensitivities as well as the covariance matrix can be computed when the derivative of $\mathbf{x}(\mathbf{v})$ from Eq. (7) with respect to $\mathbf{v}$ is known. It can be computed by implicit differentiation as follows [Wie95b]:

$$\mathbf{0} = (\sum_i \mathbf{v}_i \cdot \mathbf{P}_i) \cdot \frac{\partial \mathbf{x}}{\partial \mathbf{v}_j} + (\mathbf{x}^{\text{inp}} \cdot \mathbf{P}_j \cdot \mathbf{x} + \mathbf{P}_j^{\text{inp}})$$

Thus $\partial \mathbf{x}/\partial \mathbf{v}$ can be computed using the same matrix factorization that has already been used for computing $\mathbf{x}(\mathbf{v})$ in Eq. (10). This further emphasizes the use of direct methods instead of an iterative solution of Eq. (7) (cf. section 4.2). A similar implicit differentiation formula can be proven for the isotopomer system (9).

Finally, it should be mentioned that sensitivity analysis is only an approximative approach to statistical analysis because the originally nonlinear model is replaced by its linearization. It is well known that this can lead to serious extrapolation errors [BW88, Páz93]. Moreover it can be shown [Sie95, Wie95c] that this effect will most likely occur when large exchange fluxes are estimated. In the case where a graphical method is applicable (cf. section 4.8), nonlinear confidence regions can be immediately derived from the graphical representation [Lee93, ZS94, Wie95c]. A more general approach to estimate nonlinear parameter confidence regions that uses nonlinear statistical methods is developed in [Wie95c].

5 Global Analysis of Stationary Labeling Systems

5.1 Problems of Global System Analysis

This section concentrates on the principal amount of information that can be obtained from metabolic carbon labeling experiments. In this context the results of a parameter-fitting procedure are always unsatisfactory for various reasons:

1. Parameter-fitting produces local results, i.e. a global optimum can never be guaranteed. In [WdG93] an example from the pentose phosphate pathway has been given that admits for two alternative flux solutions both with good (local) statistical quality measures. An even more complicated example is given in [ZS94] where either one or two solutions can occur in a certain system state.

2. The result is an a posteriori result, i.e. it cannot be decided in advance (i.e. a priori) if the measurements will contain sufficient information for flux determination.

3. The measurement of fractional labels or even isotopomers is a time-consuming procedure. If redundancies in this input data can be predicted a priori this will save a lot of time because some measurements do not have to be performed.

4. Any additional a priori characterization of the experiment outcome of an experiment can be used for complexity reduction. This is of great importance when isotopomer systems are considered.

Obviously, these questions are of great importance for the design and evaluation of experiments. In the case of flux analysis from extracellular flux measurements alone we are confronted with a linear system for which all questions posed above can be explicitly and efficiently answered [VS93, vHHH+94, vHRH+94]. On the other hand label balancing introduces algebraic equations to the system so that more advanced methods have to be used for system analysis. Interestingly many questions can be answered in this situation too.

5.2 Identifiability and Redundancy

The questions posed above are better known as identifiability and redundancy problems in control engineering [Wal87]. In this context the central problems are:

Identifiability a posteriori , which means that all fluxes $\mathbf{v}$ can be uniquely determined from a given data set $(\mathbf{w}, \mathbf{y})$.

Identifiability a priori , which means that all fluxes $\mathbf{v}$ can be uniquely determined whatever the outcome $(\mathbf{w}, \mathbf{y})$ of the experiment will be.

Redundancy of measurements , which means that there exist relations $\mathbf{f}(\mathbf{w}, \mathbf{y}) = \mathbf{0}$ that hold independently of the non-measurable fluxes in $\mathbf{v}$.

In any case the measurements must be assumed to be taken without error (i.e. $\varepsilon_w = \varepsilon_y = \mathbf{0}$). This means no restriction because sensitivity can be studied later by using the methods presented in section 4.9.

It may be observed that Eqs. (8) when combined with Eq. (13) represents a general parametrized linear state space model with measured variables $\mathbf{y}$. For such models many results on identifiability have been proven [DdA87]. On the other hand the stationary case of Eq. (7) has never been considered explicitly because the number of measurements was too low to obtain significant results. This makes stationary flux identification essentially a new problem.

5.3 Algebraic Methods

Explicit and sometimes quite long-winded algebraic calculations for deriving explicit flux solutions of metabolic carbon labeling systems can be found in numerous publications [Coh83, MSJ88, Lee93, MCDB94, STM+94]. In each case the solution strategy is highly application specific and based on various simplifying assumptions on the network structure. The usual assumption is that all reaction steps are either irreversible or in rapid equilibrium [STM+94, ZS95]. Moreover whole metabolic pathways like the pentose phosphate pathway are found to be lumped to one reaction step [PSMC93, STM+94]. If any new equation is inserted in the system all computations have to be reworked and most possibly a completely new solution strategy has to be found. This will almost surely happen when exchanging reactions are added because the complexity of networks is in a close relation to the number of cyclic pathways they contain [KP92, Mes93].

A general approach to algebraic identifiability analysis presented in [Wie95a] and [Wie95b] is based on network simplification algorithms [RML93, GS91] and computer algebraic methods [CLO92, BW93] (see [FR95] for more empirical approach). The general idea is to automatically derive explicit equations relating fluxes to label measurements. In particular it can be tried to express the unknown fluxes in terms of measured quantities as has been done in section 4.4. Similar computer algebraic algorithms for multivariate polynomial equations have been successfully applied to identifiability problems in control engineering [LR87], solution of stationary biochemical reaction systems [MMN89] or stationary optimization of fermentation processes [PT95]. The details would exceed the scope of this text so that only the results that come out for the example are given here.

5.4 Analysis of the Example System

For the example system it has been already proven by Eq. (11) that all fluxes are identifiable a priori if $v_1^{\rightarrow}, v_5^{\rightarrow}$ and b_1, b_2 are known. Clearly, it follows the identifiability a posteriori. On the other hand the following redundancy relations can be proven to hold independent of the actual fluxes $v_1^{\rightarrow}, v_2^{\rightarrow}, v_2^{\leftarrow}, v_5^{\rightarrow}$:

$$\begin{aligned} 0 &= b_1e_1 - b_2^2 - b_1 + b_2 & \qquad 0 &= b_2 - b_2^2 - b_1 + b_{11} \\ 0 &= b_1e_2 - b_2e_1 - b_1 + e_1 & \qquad 0 &= b_1e_{11} - e_1b_{11} \end{aligned}$$

From this we immediately obtain

$$\begin{aligned} e_1 &= (b_2^2 + b_1 - b_2)/b_1 & \qquad b_{11} &= b_2^2 + b_1 - b_2 \\ e_2 &= (b_2e_1 + b_1 - e_1)/b_1 & \qquad e_{11} &= b_{11}e_1/b_1 \end{aligned}$$

while b_{00}, e_{00} follow from Eq. (3). Consequently, b_1 and b_2 contain all information on fluxes that can be obtained by label measurements. All the other label as well as isotopomer fractions are redundant! This example shows that isotopomer measurements need not increase the available information on intracellular fluxes as was the case in the example from section 1.8.

6 Application to *Corynebacterium glutamicum*

6.1 Example Organism and Measured Data

Corynebacterium glutamicum has always been of great interest for amino acid production, which is closely coupled to the central metabolic pathways, i.e. glycolysis, pentose phosphate pathway

and citric acid cycle. Thus stationary flux analysis is a promising diagnostic method in the context of metabolic engineering for amino acid production. The *C. glutamicum* strain MH20-22B studied in [MdGW$^+$95] is known as a lysine producer. Since in this text the focus is on the principles of flux analysis more details on the biology of this organism can be taken from [EdG95]. The following results are taken from [MdGW$^+$95].

C. glutamicum MH20-22B was cultivated under lysine producing conditions with a dilution rate of 0.1 h^{-1} in continuous culture. In this situation the total substrate uptake rate was 1.49 mmol/ (g $\cdot$ h) (dry cell mass) from which 18.3 % lysine was obtained. Table 1 presents all measured extracellular fluxes that are normed to a 100 % substrate influx for convenience. For calculating the biomass effluxes a biomass composition similar to that of [NIS90] was assumed.

Intracellular fractional labels were measured using the decoupling technique described in section 2.4. To obtain a (nearly) equilibrated labeling state in the protein fraction three cell residence times were taken for incubation with [1-^{13}C]glucose corresponding to a washout correction factor of 1.05 (cf. Eq. (1)). The separated amino acids and the corresponding label enrichment can be taken from Table 2. All measured NMR spectra have a high quality, an example is shown in Fig. 7. From these spectra a measurement error below the values given in Table 2 can be asserted.

Flux	Measured Value [%]
Substrate uptake:	
GLC	100.0
Biomass effluxes:	
G6P	1.3
F6P	0.5
GAP	0.9
PYR	18.0
PYR$\star$	23.0
E4P$\star$	1.8
RI5P	1.0
RI5P†	4.9
AKG	7.0
AKG†	1.2
OAA	11.6
Product formation:	
LYS$\star$	18.3
CO2	275.1

Table 1: Extracellular fluxes measured in continuous culture of *C. glutamicum* All values are normed to a 100 % glucose uptake rate of 1.49 mmol/ (g $\cdot$ h) (dry cell mass) Metabolite abbreviations can be taken from Fig. 13 and are assumed to be self explaining (see [MdGW$^+$95] for details). $\star$ indicates a flux coupled to CO_2 formation. † indicates a flux coupled to CO_2 refixation.

6.2 Biochemical Network

For shortness the detailed biochemical reaction equations in the formal notation introduced in section 3.2 are not reproduced here and only the underlying metabolite network used for flux estimation is presented in Fig. 13. Reaction steps that have been assumed to be bidirectional

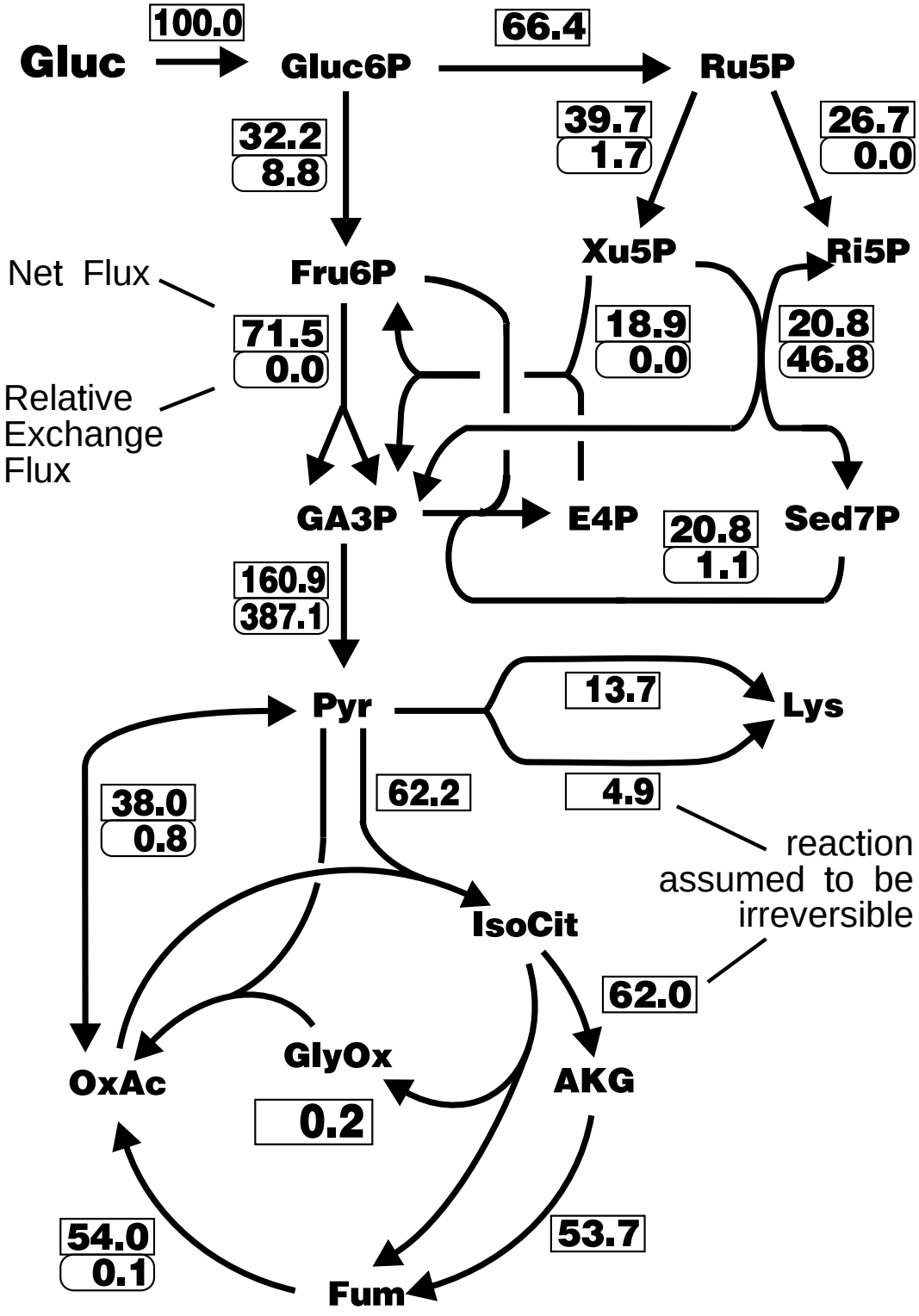

Figure 13: Biochemical network used for flux analysis in *Corynebacterium glutamicum* MH20-22B under lysine producing conditions (data from [MdGW^{+}95]). Estimated stationary net fluxes are given in rectangular boxes while the associated exchange fluxes for bidirectional reaction steps given in rounded boxes are taken relative to the corresponding net fluxes, i.e. the values v^{xch}/v^{net} are represented. Effluxes to biomass (see Table 1) have been left out for simplicity.

Carbon Atom	Measured Value [%]	Estimated Value [%]	Measurement Precision [%]
E4P#1	2.0	2.5	1.0
E4P#2	3.6	2.0	1.0
E4P#3	2.0	1.9	1.0
E4P#4	16.7	15.3	2.0
GAP#1	2.9	2.7	0.2
GAP#2	2.6	2.6	0.1
GAP#3	26.7	26.3	0.2
PYR#2	3.0	2.7	1.0
PYR#3	26.4	26.3	0.5
AKG#2	24.1	22.6	0.3
AKG#3	11.1	9.8	0.5
AKG#4	28.1	26.3	0.6
OAA#2	7.7	9.8	2.0
OAA#3	20.9	22.6	2.0
OAA#4	16.8	17.3	2.7
LYS#2	6.8	7.1	0.2
LYS#3	21.9	24.0	0.3
LYS#4	18.9	17.3	1.0
LYS#5	22.2	24.9	1.0
LYS#6	5.6	5.3	0.3
CO2#1	23.0	21.6	0.4

Table 2: Some fractional labels measured from protein hydrolysate of *C. glutamicum* compared to values predicted by the balance equations with the estimated fluxes [MdGW$^+$95]. The measurement precision depends on the quality of the measured spectra. Labeled CO_2 was measured by mass spectroscopy.

are labeled therein by an additional box with rounded edges. Irreversibility assumptions were made on the basis of thermodynamic considerations. The scrambling steps from Fig. 4 have been introduced in the citric acid cycle and in the glyoxylate shunt. Both lysine production pathways [SSK+91] have been incorporated.

A remark has to be made on the anaplerotic reaction section (cf. [Val91]). There are three possible anaplerotic reaction steps catalyzed by PEP carboxylase, PEP carboxykinase and the malic enzyme while even a fourth enzyme (pyruvate carboxylase) may be present [TMT79]. Only the PEP carboxykinase step is supposed to be reversible. The identifiability of the corresponding fluxes from label measurements has been discussed in [Wie95b]. It turned out that for the anaplerotic section only a combined net flux from the lumped phosphoenolpyruvate-pyruvate pool to the oxaloacetate pool can be estimated accompanied by an exchange flux. Interestingly, more details of anaplerotic fluxes would be identifiable if the malate labeling state were available.

6.3 Achieved Results

The intracellular flux estimates (Eq. (14)) computed from the measured data are shown in Fig. 13. Moreover the simulated labeling state corresponding to the estimates is presented in Table 2. The table shows that all label measurements are well reproduced by the simulation run. The measured fluxes are even better reproduced but are not given here for shortness. From computed statistical quality measures given in [Sie95] it becomes clear that all net fluxes are well determined. On the other hand the estimated exchange fluxes are only accurate within an order of magnitude (compare to section 4.9). However, it is possible to decide if a reaction step is highly reversible or rather unidirectional which is the principal goal of the analysis.

Some remarkable facts that are closely linked to modeling and the general stationary flux determination problem shall be pointed out. Further biological implications are discussed in [EdG95]:

1. Bidirectional reaction steps frequently occur and can be quantitated in vivo which seems to be impossible in vitro [FCA+93]. Consequently, the consideration of such steps in the modeling process is absolutely necessary. This in turn requires a large amount of measurement data for estimating all unknown parameters.

2. All fluxes are estimated without the incorporation of energy balances. Thus results on the cellular energy metabolism can be derived from the achieved quantitative results. For example it turns out that there is an excess NADHP formation for which a consuming reaction is not yet known [MdGW+95]. A balanced NADPH formation was previously assumed in [Val91].

3. The exchange rate of the anaplerotic reaction section indicates a futile cycle which once more stresses the importance of bidirectional reactions (cf. [dHBS81, CMCM+94]).

7 Conclusion and Future Prospects

Stationary flux determination is proven to be an invaluable diagnostic tool in the context of metabolic engineering. When sufficient measurement data is available it can be carried out with almost no critical assumptions on the living system like e.g. energy balancing. For this purpose fractional labeling data from carbon tracer experiments is an important source of information in

addition to direct extracellular flux measurements. Using this source enables not only net fluxes to be estimated but also exchange fluxes of bidirectional reaction steps. These in turn allow to distinguish between equilibrating and irreversible reaction steps in vivo. This was illustrated successfully for the complete central metabolism of *C. glutamicum* in [MdGW$^+$95]. If isotopomer measurements are available this may even increase the amount of information but it need not to be so in every case.

From general modeling considerations it becomes clear that as many information sources as possible should be used for flux determination. In this context isotopomer measurements are a promising source of information that is currently not extensively used. Modeling and data analysis with isotopomer systems will require additional efforts for solving the associated high dimensional numerical problems. The same holds for the statistical analysis of the estimated parameters which poses a difficult nonlinear statistical problem [Sie95]. Finally, from the viewpoint of global system analysis, general methods for network reduction, identifiability and redundancy analysis have to be developed that allow to judge the amount of information that can be achieved with a certain experiment. Finally appropriate software tools for stationary flux analysis are required when this technique is to be established in interdisciplinary research teams [Wie94a, Wie95d].

From the experimental viewpoint the measurement procedures have to be further accelerated to establish stationary flux analysis by ^{13}C tracer experiments as a routine procedure. Only the evaluation of a series of experiments under varied physiological conditions can bring a true insight into metabolic regulation [VS93, Jor95, SSdG$^+$95]. Similarly, the comparison of different strains which are distinguished by well known genetic modifications will demonstrate the role of a certain enzymatic step within a complex network. Finally, stationary flux analysis — being free from assumptions on the biological system to a large degree — may help to find out how enzymes really work in vivo, i.e. phenomena like channeling, enzyme complexes or scrambling [Mat93, SSMS93] may be investigated in more detail when sufficient measurement information is available.

References

[And83] D.H. Anderson. *Compartmental Modelling and Tracer Kinetics*, volume 50 of *Lecture Notes in Biomathematics*. Springer, 1983.

[Arn90] S.F. Arnold. *Mathematical Statistics*. Prentice Hall, 1990.

[AW92] K.R. Albe and B.E. Wright. Systems analysis of the tricarboxylic acid cycle in *dictyostelium discoideum*: II. control analysis. *J. Biol. Chem.*, 267:3106–3114, 1992.

[Bai91] J.E. Bailey. Towards a science of metabolic engineering. *Science*, 252:1668–1674, 1991.

[BD85] G.C. Barrett and J.S. Davies. *Nuclear Magnetic Resonance Spectra of Amino Acids and their Derivatives*, chapter 18. Chapman and Hall, 1985.

[BL94] D. Bray and S. Lay. Rapid numerical integration algorithm for finding the equilibrium state of a system of coupled binding reactions. *Computer Applications in the Biosciences*, 10(5):471–476, 1994.

[BS82] J.J. Blum and R.B. Stein. On the analysis of metabolic networks. In R.F. Goldberger, editor, *Biological Regulation and Development*, volume 3A, chapter 3, pages 99–124. Plenum Press, 1982.

[BW88] D.M. Bates and D.G. Watts. *Nonlinear Regression Analysis and its Applications*. Probability and Mathematical Statistics. Applied Probability and Statistics. Wiley, 1988.

[BW93] T. Becker and V. Weispfennig. *Gröbner Bases — A computational Approach to Commutative Algebra*, volume 141 of *Graduate Texts in Mathematics*. Springer, 1993.

[CB83] J.M. Crawford and J.J. Blum. Quantitative analysis of flux along the gluconeogenic, glycolytic and pentose phosphate pathways under reducing conditions in hepatocytes isolated from fed rats. *Biochem. J.*, 212:595–598, 1983.

[CB95] M. Cohen and R.N. Bergman. Estimation of TCA cycle flux, aminotransferase flux, and anaplerosis in heart: validation with syntactic model. *Am. J. Physiol.*, 268:E397–E409, 1995.

[CF80] J.-P. Chambost and D.G. Fraenkel. The use of 6-labeled glucose to assess futile cycling in *escherichia coli*. *J. Biol. Chem.*, 255:2867–2869, 1980.

[CFGC95] J.C. Chatham, J.R. Forder, J.D. Glickson, and E.M. Chance. Calculation of absolute metabolic fluxes and the elucidation of the pathways of glutamate labeling in perfused rat heart by ^{13}C NMR spectroscopy and nonlinear least squares analysis. *The Journal of Biological Chemistry*, 270:7999–8008, 1995.

[CL94] Y.-P. Chao and J.C Liao. Metabolic responses to substrate futile cycling in escherichia coli. *J. Biol. Chem.*, 269:5122–5126, 1994.

[CLO92] D. Cox, J. Little, and D. O'Shea. *Ideals, Varieties and Algorithms — An Introduction to Computational Algebraic Geometry and Commutative Algebra*. Undergraduate Texts in Mathematics. Springer, 1992.

[CMCM+94] M.-F. Chauvin, F. M gnin-Chanet, G. Martin, J.-M. Lhoste, and G. Baverel. The rabbit kidney tubule utilizes glucose for glutamine synthesis. *J. Biol. Chem.*, 269:26025–26033, 1994.

[Coh83] S.M. Cohen. Simultaneous ^{13}C and ^{31}P NMR studies of perfused rat liver. *J. Biol. Chem.*, 258:14294–14308, 1983.

[CRSK81] S.M. Cohen, R. Rognstad, R.G. Shulman, and J. Katz. A comparison of ^{13}C nuclear magnetic resonance and ^{14}C tracer studies of hepatic metabolism. *J. Biol. Chem.*, 256:3428–3432, 1981.

[CSKW83] E.M. Chance, S.H. Seeholzer, K. Kobayashi, and J.R. Williamson. Mathematical analysis of isotope labeling in the citric acid cycle with applications to ^{13}C NMR studies in perfused rat hearts. *J. Biol. Chem.*, 258:13785–13794, 1983.

[DAM88] Dori, Arato, and Maga. Determination of unresolved peaks via a new non linear regression procedure. *Annali di chimica*, 78:529–542, 1988.

[DdA87] J. Delforge, L. d'Angio, and S. Audoly. Results and conjectures on the identifiability of linear systems. In Walter [Wal87], chapter 2, pages 21–31.

[Deu95] P. Deuflhard. *Newton Methods for Highly Nonlinear Problems: Theory, Algorithms, Code*. Academic Press, 1995. To appear.

[dGWP+92] A.A. de Graaf, R.M. Wittig, U. Probst, J. Strohhäcker, S.M. Schoberth, and H. Sahm. Continuous-flow NMR bioreactor for *in vivo* studies of microbial cell suspensions with low biomass concentrations. *Journal of Magnetic Resonance*, 98:654–659, 1992.

[dHBS81] J.A. den Hollander, K.L. Behar, and R.G. Shulman. ^{13}C NMR study of transamination during acetate utilization by *saccharomyces cerevisiae. Proc. Natl. Acad. Sci.*, 78:2693–2697, 1981.

[dHUB+86] J.A. den Hollander, K. Ugurbil, T.R. Brown, M. Bednar, C.Redfield, and R.G. Shulman. Studies of anaerobic and aerobic glycolysis in *saccharomyces cerevisiae*. *Biochemistry*, 25:203–211, 1986.

[DLC+84] M.M. Domach, S.K. Leung, R.E. Cahn, C.G. Cocks, and M.L. Shuler. Computer model for glucose-limited growth of a single cell of *eschericia coli* b/r-a. *Biotechn.Bioeng.*, 26:203–216, 1984.

[DRM+93] L. Di Donato, C. Des Rosiers, J.A. Montgomery, F. David, M. Garneau, and H. Brunengraber. Rates of gluconeogenesis and citric acid cycle in perfused livers, assessed from the mass spectrometric assay of the ^{13}C labeling pattern of glutamate. *The Journal of Biological Chemistry*, 268(6):4170–4180, 1993.

[EdG95] L. Eggeling and A.A. de Graaf. Quantifying and directing metabolite flux: Application to amino acid overproduction. *Advances in Biochemical Engineering/Biotechnology*, 1995. This volume.

[ESS83] I. Ekiel, I.C.P. Smith, and G.D. Sprott. Biosynthetic pathways in *methanospirillum hungatei* as determined by ^{13}C nuclear magnetic resonance. *J. Bacteriol.*, 156:316–326, 1983.

[ESW+93] W. Eisenreich, G. Strauss, U. Werz, G. Fuchs, and A. Bacher. Retrobiosynthetic analysis of carbon fixation in the phototrophic eubacterium *chloroflexus aurantiacus*. *Eur. J. Biochem.*, 215:619–632, 1993.

[FCA+93] I. Flanigan, J.G. Collins, K.K. Arora, J.K. MacLeod, and J.F. Williams. Exchange reactions catalysed by group-transferring enzymes oppose quantitation and the unravelling of the identity of the pentose phosphate pathway. *Eur.J.Biochem.*, 213:477–485, 1993.

[FHBS90] S.M. Fitzpatrick, H.P. Hetherington, K.L. Behar, and R.G. Shulman. The flux from glucose to glutamate in the rat brain in vivo as determined by ^{1}H-observed, ^{13}C-edited NMR spectroscopy. *J. Cerebr. Blood Flow Metab.*, 10:170–179, 1990.

[FR95] C.A. Fernandez and C. Des Rosiers. Modeling of liver citric acid cycle and gluconeogenesis based on ^{13}C mass isotopomer distribution analysis of intermediates. *J. Biol. Chem.*, 270:10037–10042, 1995.

[Gad82] D.G. Gadian. *Nuclear Magnetic Resonance and its Application to Living Systems.* Oxford University Press, 1982.

[GFJA93] A. Goel, J. Ferrance, J. Jeong, and M.M. Ataai. Analysis of metabolic fluxes in batch and continuous cultures of *bacillus subtilis*. *Biotechnology and Bioengineering*, 42:686–696, 1993.

[GS91] G. Gielen and W. Sansen. *Symbolic Analysis for Automated Design of Analog Integrated Circuits.* Kluwer Academic Publishers, 1991.

[Hac93] W. Hackbusch. *Iterative Lösung großer schwachbesetzter Gleichungssysteme.* Number 69 in LAMM. Teubner Verlag, 1993.

[Har95] A. Hartbrich. *Verfahrenstechnische Charakterisierung von Zyklonreaktoren in der Biotechnologie*. PhD thesis, RWTH Aachen, 1995.

[HNW87] E. Hairer, S.P. Norsett, and G. Wanner. *Solving Ordinary Differential Equations I — Nonstiff Problems*, volume 8 of *Series in Computational Mathematics.* Springer, 1987.

[Hof86] J.H.S. Hofmeyr. Steady-state modelling of metabolic pathways: a guide for the prospective simulator. *CABIOS*, 2(1):5–11, 1986.

[Hof93] R. Hofestädt. Grammatical formalization of metabolic processes. In Hunter et al. [HSS93], pages 181–189.

[Hol86] W.H. Holms. The central metabolic pathways of escherichia coli: relationship between flux and control at a branch point, efficiency of conversion to biomass, and excretion of acetate. *Curr. Topics Cell. Regul.*, 28:69–104, 1986.

[HS93] H.G. Holzhütter and A. Schwendel. Estimation of enzymatic flux rates from kinetic isotope experiments. In Schuster et al. [SROM93].

[HSG+93] H.-G. Holzhütter, A. Schwendel, T. Grune, J. Quedenau, and W. Siems. Estimation of steady-state flux rates in metabolic systems by computer simulations of radioactive tracer exeriments. *CABIOS*, 9(5):573–580, 1993.

[HSS93] L. Hunter, D. Searls, and J. Shavlik, editors. *ISMB-93, Proceedings of the First International Conference on Intelligent Systems for Molecular Biology*. AAAI Press, 1993.

[HW91] E. Hairer and G. Wanner. *Solving Ordinary Differential Equations II — Stiff and Differential-Algebraic Problems*, volume 14 of *Series in Computational Mathematics*. Springer, 1991.

[IL87] L. Inbar and A. Lapidot. ^{13}C-NMR, ^{1}H-NMR and gas-chromatography mass-spectrometry studies of the biosynthesis of ^{13}C-enriched L-lysine by *brevibacterium flavum*. *Eur. J. Biochem.*, 162:621–633, 1987.

[Jor95] H. Jorgensen. Metabolic flux distributions in penicillium chrysogenum during fed-batch cultivations. *Biotech. Bioeng.*, 46:117–131, 1995.

[JRMS91] F.M.H. Jeffrey, A. Rajagopal, C.R. Malloy, and A.D. Sherry. ^{13}C-NMR: a simple yet comprehensive method for analysis of intermediary metabolism. *TIBS*, 16:5–10, 1991.

[JSJ+93] J.G. Jones, A.D. Sherry, F.M.H. Jeffrey, C.J. Storey, and C.R. Malloy. Sources of acetyl-CoA entering the tricarboxylic acid cycle as determined by analysis of succinate ^{13}C isotopomers. *Biochemistry*, 32:12240–12244, 1993.

[JWBL89] A.W.H. Jans, C. Winkel, L. Buitenhuis, and J. Lugtenburg. ^{13}C-n.m.r. study of citrate metabolism in rabbit renal proximal-tubule cells. *Biochemical Journal*, 257:425–429, 1989.

[KA93] H. Kacser and L. Acerenza. A universal method for achieving increases in metabolite production. *European Journal of Biochemistry*, 216:361–367, 1993.

[Kac88] H. Kacser. Regulation and control of metabolic pathways. In M.J. Bazin and J.I. Prosser, editors, *Physiological Models in Microbiology*, volume 2 of *CRC Series in Mathematical Models in Microbiology*, chapter 1, pages 1–23. CRC Press, 1988.

[KC83] P.W. Kuchel and B.E. Chapman. NMR spin exchange kinetics at equilibrium in membrane transport and enzyme systems. *J.Theor.Biol.*, 105:569–589, 1983.

[KCS93] B. Künnecke, S. Cerdan, and J. Seelig. Cerebral metabolism of (1,2-$^{13}C_2$)glucose and (U-$^{13}C_4$)3-hydroxybutyrate in rat brain as detected by ^{13}C NMR spectroscopy. *NMR in Biomedicine*, 6:264–277, 1993.

[KKW79] P. Kelly, J.K. Kelleher, and B.E. Wright. The tricarboxylic acid cycle in *dictyostelium discoideum* — metabolite concentrations, oxygen uptake and ^{14}C-labelled amino acid labelling patterns. *Biochem. J.*, 184:581–588, 1979.

[KP92] D.T. Kincaid and R. Pilette. Construction of simple pathways and simple cycles in ecosystems. *Computer Applications in the Biosciences*, 8(3):267–273, 1992.

[KW86] D.B. Kell and H.V. Westerhoff. Metabolic control theory: its role in microbiology and biotechnology. *FEMS Microbiology Reviews*, 39:305–320, 1986.

[KWL93] J. Katz, P. Wals, and W.-N.P. Lee. Isotopomer studies of gluconeogenesis and the krebs cycle with ^{13}C-labeled lactate. *J. Biol. Chem.*, 268:25509–25521, 1993.

[KWR88] K. Kanamori, R.L. Weiss, and D. Roberts. Glutamate biosynthesis in *bacillus azotofixans* – ^{15}N NMR and enzymatic studies. *The Journal of Biological Chemistry*, 263(6):2871–2823, 1988.

[Lee93] W.-N.P. Lee. Analysis of tricarboxylic acid cycle using mass isotopomer ratios. *J. Biol. Chem.*, 268:25522–25526, 1993.

[LHHV90] P. Lundberg, E. Harmsen, C. Ho, and H.J. Vogel. Nuclear magnetic resonance studies of cellular metabolism. *Anal. Biochem.*, 191:193–222, 1990.

[Lon88] R.E. London. ^{13}C labeling in studies of metabolic regulation. *Prog. NMR Spectroscopy*, 20:337–383, 1988.

[Lon92] R.E. London. In vivo ^{2}H NMR studies of cellular metabolism. In L.J. Berliner and J. Reuben, editors, *Biological Magnetic Resonance*, volume 11, chapter 6, pages 277–306. Plenum Press, 1992.

[LR83] R.M. Lambrecht and A. Rescigno, editors. *Tracer Kinetics and Physiological Modelling*. Number 48 in Lecture Notes in Biomathematics. Springer, 1983.

[LR87] Y. Lecourtier and A. Raksanyi. The testing of structural properties through symbolic computation. In Walter [Wal87], chapter 7, pages 75–84.

[Mar94] A. Marx. Charakterisierung des Zentralstoffwechsels bei *corynebacterium glutamicum* mittels Metabolitbilanzierung und computergestützter Analyse von ^{13}C-NMR-Markierungsdaten. Diploma Thesis, Universität Bonn, 1994.

[Mat82] N.A. Matwiyoff. Recent applications of ^{13}C NMR spectroscopy to biological systems. In Schmidt et al. [SFH82], pages 573–585.

[Mat93] C.K. Mathews. The cell: Bag of enzymes or network of channels? *Journal of Bacteriology*, 175(20):6377–6381, 1993.

[Mav93] M.L. Mavrovouniotis. Identification of localized and distributed bottlenecks in metabolic pathways. In Hunter et al. [HSS93], pages 275–283.

[MBW94] W.J. Malaisse, M. Biesemans, and R. Willem. Mathematical modelling for the generation of L-[3-^{2}H, 3-^{13}C]lactic acid isotopomers by erythrocytes exposed to either D-[1-^{13}C]glucose or D-[6-^{13}C]glucose in the presence of $^{2}H_2O$. *Mol. Cell. Biochem.*, 130:129–136, 1994.

[MCDB94] G. Martin, M.-F. Chauvin, S. Dugelay, and G. Baverel. Non-steady state model applicable to NMR studies for calculating flux rates in glycolysis, gluconeogenesis, and citric acid cycle. *J. Biol. Chem.*, 269:26034–26039, 1994.

[MdGW+95] A. Marx, A.A. de Graaf, W. Wiechert, L. Eggeling, and H. Sahm. Determination of the fluxes in central metabolism of *corynebacterium glutamicum* by nmr spectroscopy combined with metabolite balancing. *Biotechnology and Bioengineering*, 1995. In Press.

[Mes93] G. Meszéna. Path analysis in general control theory. In Schuster et al. [SROM93].

[MMN89] H. Melenk, H.M. Möller, and W. Neun. Symbolic solution of large stationary chemical kinetic problems. *Impact of Computing in Science and Engineering*, 1(2), 1989.

[MN91] C.A. Marinov and P. Neittanmäki. *Mathematical Models in Circuit Theory: Theory and Applications.* Kluwer Academic Publishers, 1991.

[MSJ88] C.R. Malloy, A.D. Sherry, and F.M.H. Jeffrey. Evaluation of carbon flux and substrate selection through alternate pathways involving the citric acid cycle of the heart by ^{13}C NMR spectroscopy. *The Journal of Biological Chemistry*, 263(15):6964–6971, 1988.

[MSS90] M.L. Mavrovouniotis, G. Stephanopoulos, and G. Stephanopulos. Computer-aided synthesis of biochemical pathways. *Biotechnology & Bioengineering*, 36:1119–1132, 1990.

[MTBK89] L.M. McIntyre, D.R. Thorburn, W.A. Bubb, and P.W. Kuchel. Comparison of computer simulations of the F-type and L-type non-oxidative hexose monophosphate shunts with ^{31}P experimental data from human erythrocytes. *Eur.J.Biochem.*, 180:399–420, 1989.

[MTG94] D. Massiot, H. Thiele, and A. Germanus. Winfit – a windows-based program for lineshape analysis. *Bruker Report*, pages 43–46, 1994.

[NIS90] F.C. Neidhardt, J.L. Ingraham, and M. Schaechter. *Physiology of the Bacterial Cell — A Molecular Approach*. Sinauer Associates, 1990.

[NS89] F. Ni and H.A. Scheraga. Constrained iterative spectral deconvolution with applications in NMR spectroscopy. *Journal of Magnetic Resonance*, 82:413–418, 1989.

[Oku94] K. Okuno. A new cultivation system operated under a super high magnetic field. *J. Ferment. Bioeng.*, 77:453–456, 1994.

[O'L82] M.H. O'Leary. Heavy-atom isotope effects on enzyme-catalyzed reactions. In Schmidt et al. [SFH82], pages 67–75.

[Pat92] R. Patnaik. Stimulation of glucose catabolism in escherichia coli by a potential futile cycle. *J. Bac.*, 174:7527–7532, 1992.

[Páz93] A. Pázman. *Nonlinear Statistical Models.* Number 254 in Mathematics and its Applications. Kluwer Academic Publishing, 1993.

[PFTV88] W.H. Press, B.P. Flannery, S.A. Teukolsky, and W.T. Vetterling. *Numerical Recipes in C - The Art of Scientific Computing*. Cambridge University Press, 1988.

[PSMC93] J.-C. Portais, R. Schuster, M. Merle, and P. Canioni. Metabolic flux determination in C6 glioma cells using carbon-13 distribution upon [1-^{13}C] glucose incubation. *Eur. J. Biochem.*, 217:457–468, 1993.

[PT95] C. Posten and B. Tibken. Application of algebraic methods to the calculation of steady states in continuous cultures. *Control Engineering Practice*, 3(7), 1995.

[PWK94] M.W. Pickett, M.P. Williamson, and D.J. Kelly. An enzyme and ^{13}C-NMR study of carbon metabolism in heliobacteria. *Photosynth. Res.*, 41:75–88, 1994.

[RB85] M. Rabkin and J.J. Blum. Quantitative analysis of intermediary metabolism in hepatocytes incubated in the presence and absence of glucagon with a substrate mixture containing glucose, ribose, fructose, alanine and acetate. *Biochem. J.*, 225:761–786, 1985.

[RCRL90] M.F. Roberts, B.-S. Choi, D.E. Robertson, and S. Lesage. Free amino acid turnover in methanogens measured by ^{15}N NMR spectroscopy. *The Journal of Biological Chemistry*, 265(30):18207–18212, 1990.

[RDC+95] C. Des Rosiers, L. Di Donatos, B. Comte, A. Laplante, C. Marcoux, F. David, C.A. Fernandez, and H. Brunengraber. Isotopomer analysis of citric acid cycle and gluconeogenesis in rat liver — reversibility of isocitrate dehydrogenase and involvement of ATP-citrate lyase in gluconeogenesis. *J. Biol. Chem.*, 270:10027–10036, 1995.

[Red88] C. Reder. Metabolic control theory: A structural approach. *J.Theor.Biol.*, 135:175–201, 1988.

[RKBY94] B.D. Ross, P.B. Kingsley, and O. Ben-Yoseph. Measurement of pentose phosphate-pathway activity in a single incubation with [1,6-$^{13}C_2$,6,6-$^{2}H_2$]glucose. *Biochem.J.*, 302:31–38, 1994.

[RML93] V.N. Reddy, M.L. Mavrovouniotis, and M.N. Liebman. Petri net representations in metabolic pathways. In Hunter et al. [HSS93], pages 328–336.

[Roe83] J.A. Roels. *Energetics and Kinetics in Biotechnology*. Elsevier Biomedical Press, 1983.

[SB79] R.B. Stein and J.J. Blum. Quantitative analysis of intermediary metabolism in *tetrahymena* — cells grown in proteose-peptone and resuspended in a defined nutrient-rich medium. *J. Biol. Chem.*, 254:10385–10395, 1979.

[SB88] J. Vanni Shanks and E. Bailey. Estimation of intracellular sugar phosphate concentrations in *saccharomyces cerevisiae* using ^{31}P nuclear magnetic resonance spectroscopy. *Biotechnology and Bioengineering*, 32:1138–1152, 1988.

[Sch91] K. Schügerl, editor. *Biotechnology, Vol.4: Measuring, Modelling and Control*. Verlag Chemie, 2 edition, 1991.

[Sch95] V. Schwingenheuer. Redundanzanalyse bei metabolischen Kohlenstoff-Markierungssystemen. Diploma Thesis, Universität Bonn, 1995.

[SEBF92] G. Strauss, W. Eisenreich, A. Bacher, and G. Fuchs. ^{13}C-NMR study of autotrophic CO_2 fixation pathways in the sulfur-reducing archaebacterium *thermoproteus neutrophilus* and in the phototrophic eubacterium *chloroflexus aurantiacus*. *Eur. J. Biochem.*, 205:853–866, 1992.

[SEdGS93] K. Sonntag, L. Eggeling, A.A. de Graaf, and H. Sahm. Flux partitioning in the split pathway of lysine synthesis in *corynebacterium glutamicum* — quantification by ^{13}C- and ^{1}H-NMR spectroscopy. *European Journal of Biochemistry*, 213:1325–1331, 1993.

[Seg75] I.H. Segel. *Enzyme Kinetics: Behaviour and Analysis of Rapid-Equilibrium and Steady-State Enzyme Systems*. Wiley, 1975.

[SFH82] H.-L. Schmidt, H. Förstel, and K. Heinzinger, editors. *Stable Isotopes, Proceedings of the 4th International Conference, Jülich, March 23-26, 1981*, volume 11 of *Analytical Chemistry Symposia Series*. Elsevier, 1982.

[Sie95] C. Siefke. Ein numerisches Verfahren zur Flu schätzung bei metabolischen ^{13}C-Markierungsexperimenten. Diploma Thesis, Universität Bonn, 1995.

[SM95] K. Schuegerl and A. Munack, editors. *3rd IFAC Symposium on Modelling and Control of Biotechnical Processes, Garmisch-Partenkirchen, 1995*. Pergamon Press, 1995.

[SROM93] S. Schuster, M. Rigoulet, R. Ouhabi, and J.-P. Mazat, editors. *Modern Trends in Biothermokinetics — Proc. 5th Int. Meeting on Biothermokinetics, Sept. 23-26, Bordeaux, France.* Plenum, 1993.

[SS93] G. Stephanopoulos and A.J. Sinskey. Metabolic engineering - methodologies and future prospects. *TibTech*, 11:392–396, 1993.

[SSdG+95] K. Sonntag, J. Schwinde, A.A. de Graaf, A. Marx, B.J. Eikmanns, W. Wiechert, and H. Sahm. ^{13}C NMR studies of the fluxes in the central metabolism of *corynebacterium glutamicum* during growth and overproduction of amino acids in batch cultures. *Applied Microbiology and Biotechnology*, 1995. In press.

[SSH92] R. Schuster, S. Schuster, and H.-G. Holzhütter. Simplification of complex kinetic models used for the quantitative analysis of nuclear magnetic resonance or radioactive tracer studies. *J.Chem.Soc. Faraday Trans.*, 88(19):2837–2844, 1992.

[SSK+91] B. Schrumpf, A. Schwarzer, J. Kalinkowski, A. Pühler, L. Eggeling, and H. Sahm. A functionally split pathway for lysine synthesis in *c. glutamicum*. *Journal of Bacteriology*, 173(14):4510–4516, 1991.

[SSMS93] B. Sumegi, A.D. Sherry, C.R. Malloy, and P.A. Srere. Evidence for orientation-conserved transfer in the TCA cycle in *saccharomyces cerevisiae*: ^{13}C NMR studies. *Biochem.*, 32:12725–12729, 1993.

[STM+94] S.T. Sharfstein, S.N. Tucker, A. Mancuso, H.W. Blanch, and D.S. Clark. Quantitative in vivo nuclear magnetic resonance studies of hybridoma metabolism. *Biotechnology and Bioengineering*, 43:1059–1074, 1994.

[SV91] G. Stephanopoulos and J.J. Vallino. Network rigidity and metabolic engineering in metabolite overproduction. *Science*, 252:1675–1681, 1991.

[SW89] G.A.F. Seber and C.J. Wild. *Nonlinear Regression.* Wiley, 1989.

[TDHW91] S. Tran-Dinh, M. Herve, and J. Wietzerbin. Determination of flux through different metabolite pathways in *saccharomyces cerevisiae* by ^{1}H-NMR and ^{13}C-NMR spectroscopy. *European Journal of Biochemistry*, 201:715–721, 1991.

[TMT79] O. Tosaka, H. Morioka, and K. Takinami. The role of biotin dependent pyruvate carboxylase in l-lysine production. *Agric.Biol.Chem.*, 43:1513–1519, 1979.

[Val91] J.J. Vallino. *Identification of Branch-Point Restrictions in Microbial Metabolism through Metabolic Flux Analysis and local Network Perturbations.* PhD thesis, Massachusetts Institute of Technology, 1991.

[vHHH+94] R.T.J.M. van Heijden, J.J. Heijnen, C. Hellinga, B. Romein, and K.C.A.M. Luyben. Linear constraint relations in biochemical reaction systems: I. classification of the calculability and the balanceability of conversion rates. *Biotechnology and Bioengineering*, 43:3–10, 1994.

[vHRH+94] R.T.J.M. van Heijden, B. Romein, J.J. Heijnen, C. Hellinga, and K.C.A.M. Luyben. Linear constraint relations in biochemical reaction systems: Ii. diagnosis and estimation of gross errors. *Biotechnology and Bioengineering*, 43:11–20, 1994.

[VP94a] A. Varma and B.O. Palsson. Metabolic flux balancing: basic concepts, scientific and practical use. *Bio/Technol.*, 12:994–998, 1994.

[VP94b] A. Varma and B.O. Palsson. Stoichiometric flux balance models quantitatively predict growth and metabolic by-product secretion in wild-type escherichia coli w3110. *Appl. Env. Microbiol.*, 60:3724–3731, 1994.

[VS93] J.J. Vallino and G. Stephanopoulos. Metabolic flux distribution in *corynebacterium glutamicum* during growth and lysine overproduction. *Biotechnology and Bioengineering*, 41:633–646, 1993.

[Wal87] E. Walter, editor. *Identifiability of Parametric Models.* Pergamon, 1987.

[WBA92] B.E. Wright, M.H. Butler, and K.R. Albe. Systems analysis of the tricarboxylic acid cycle in *dictyostelium discoideum*: I. the basis for model construction. *J. Biol. Chem.*, 267:3101–3105, 1992.

[WdG93] W. Wiechert and A.A. de Graaf. Modelling of ^{13}C labelling in metabolic pathways for in vivo flux analysis using NMR. In V. Bales, editor, *Modelling for improved Bioreactor Performance, EFB Working Party on Bioreactor Performance, 27.-28. September 1993, Papiernicka, Slovakia*, pages 19–24. Malé Centrum, Publisher & Bookshop, Bratislava, 1993.

[WdG95] D. Weuster and A.A. de Graaf. Reaction engineering methods to study intracellular metabolite concentrations. *Advances in Biochemical Engineering/Biotechnology*, 1995. This volume.

[WdGA95] W. Wiechert, A.A. de Graaf, and A.Marx. In vivo stationary flux determination using ^{13}C NMR isotope labelling experiments. In Schuegerl and Munack [SM95]. In Press.

[WGKF+92] R.G. Weiss, S.T. Gloth, R. Kalil-Filho, V.P. Chacko, M.D. Stern, and G. Gerstenblith. Indexing tricarboxylic acid cycle flux in intact hearts by carbon-13 nuclear magnetic resonance. *Circ. Res.*, 70:392–408, 1992.

[WHK+82] T.E. Walker, C.H. Han, V.H. Kollman, R.E. London, and N.A. Matwiyoff. ^{13}C nuclear magnetic resonance studies of the biosynthesis by *microbacterium ammoniaphilum* of L-glutamate selectively enriched with carbon-13. *J. Biol. Chem.*, 257:1189–1195, 1982.

[Wie94a] W. Wiechert. Design of a software framework for flux determination by ^{13}C NMR isotope labelling experiments. In E. Gnaiger, F.N. Gellerich, and M. Wyss, editors, *What is Controlling Life?*, volume 3 of *Modern Trends in BioThermoKinetics*. Innsbruck University Press, 1994.

[Wie94b] W. Wiechert. Diskrete Analyse von Stoffwechselnetzwerken. In F. Haubensack and J. Sühnel, editors, *Bioinformatik — Computereinsatz in den Biowissenschaften*, pages 100–111. Institut für Molekulare Biotechnologie, Jena, Available on Internet: ftp.imb-jena.de, 1994.

[Wie95a] W. Wiechert. Algebraic methods for the analysis of redundancy and identifiability in metabolic ^{13}C labelling systems. In Schomburg, editor, *3. Fachtagung Bioinformatik, Braunschweig*, 1995.

[Wie95b] W. Wiechert. Metabolic flux determination by stationary ^{13}C tracer experiments: Analysis of sensitivity, identifiability and redundancy. In Dolezal, editor, *IFIP TC7, Conference on System Modelling and Optimization*. Chapman and Hall, 1995.

[Wie95c] W. Wiechert. Metabolische Kohlenstoff-Markierungssysteme — Modellierung, Simulation und Analyse. Habilitationsschrift, Universität Bonn, 1995.

[Wie95d] W. Wiechert. Object oriented programming for the biosciences. *Computer Applications in the Biosciences*, 1995. In Press.

[WK84] K. Walsh and D.E. Koshland. Determination of flux through the branch point of two metabolic cycles — the tricarboxylic acid cycle and the glyoxylate shunt. *J. Biol. Chem.*, 259:9646–9654, 1984.

[WKKS82] F.J. Winkler, H. Kexel, C. Kranz, and H.-L. Schmidt. Parameters affecting the $^{13}CO_2/^{12}CO_2$ discrimination of the ribulose-1,5-bisphosphate carboxylase reaction. In Schmidt et al. [SFH82], pages 83–89.

[WMWdG95] R. Wittig, M. Möllney, W. Wiechert, and A.A. de Graaf. Interactive evaluation of nmr spectra from in vivo isotope labelling experiments. In Schuegerl and Munack [SM95]. In Press.

[Wol82] M. Wolfsberg. The theoretical analysis of isotope effects. In Schmidt et al. [SFH82], pages 3–14.

[WvD87] H.V. Westerhoff and K. van Dam. *Mosaic Nonequilibrium Thermodynamics and Control of biological Free-Energy Transduction.* Elsevier Amsterdam, 1987.

[ZS94] C. Zupke and G. Stephanopoulos. Modeling of isotope distributions and intracellular fluxes in metabolic networks using atom mapping matrices. *Biotechnol. Prog.*, 10:489–498, 1994.

[ZS95] C. Zupke and G. Stephanopoulos. Intracellular flux analysis in hybridomas using mass balances and in vitro ^{13}C NMR. *Biotechn. Bioeng.*, 45:292–303, 1995.